NATIONAL ADVISORY COMMITTEE FOR AERONAUTICS

TECHNICAL NOTE 3467

EFFECT OF INTERACTION ON LANDING-GEAR BEHAVIOR AND DYNAMIC LOADS IN A FLEXIBLE AIRPLANE STRUCTURE

By Francis E. Cook and Benjamin Milwitzky

Langley Aeronautical Laboratory
Langley Field, Va.

Washington
August 1955

NATIONAL ADVISORY COMMITTEE FOR AERONAUTICS

TECHNICAL NOTE 3467

EFFECT OF INTERACTION ON LANDING-GEAR BEHAVIOR AND DYNAMIC LOADS IN A FLEXIBLE AIRPLANE STRUCTURE

By Francis E. Cook and Benjamin Milwitzky

SUMMARY

The effects of interaction between a landing gear and a flexible airplane structure on the behavior of the landing gear and the loads in the structure have been studied by treating the equations of motion of the airplane and the landing gear as a coupled system. The landing gear is considered to have nonlinear characteristics typical of conventional gears, namely, velocity-squared damping, polytropic air-compression springing, and exponential tire force-deflection characteristics. For the case where only two modes of the structure are considered, an equivalent three-mass system is derived for representing the airplane and landing-gear combination, which may be used to simulate the effects of structural flexibility in jig drop tests of landing gears.

As examples to illustrate the effects of interaction, numerical calculations, based on the structural properties of two large airplanes having considerably different mass and flexibility characteristics, are presented. For the particular cases considered, it was found that the effects of interaction can result in appreciable reductions in the magnitude of the landing-gear force, particularly when the flexibility of the airplane structure is large and the natural frequency is small. Thus, neglect of interaction effects, that is, the use of the landing-gear forcing function for a rigid airplane, in a dynamic analysis of a flexible airplane can lead to the calculation of excessive loads in the airplane structure.

In the case of one of the airplanes considered, the structural loads calculated from the interaction solutions are greater than those for a completely rigid airplane treatment (rigid structure subjected to rigid-body forcing function) because the effects of dynamic magnification more than overcome the reduction in landing-gear force due to interaction. In the case of the second airplane, because of the relatively large natural period of the structure in comparison with the duration of the impact pulse, the dynamic magnification factor is appreciably less than unity. This effect, coupled with the reductions in landing-gear force due to interaction, results in structural loads that are less than those for a rigid airplane.

INTRODUCTION

In the design of landing gears it is usually assumed that the airplane is a rigid body and development tests are frequently carried out in a drop-test jig with a landing gear attached to a concentrated mass. In so doing, it is tacitly assumed that the interaction between the motions of the landing gear and the deformations of the airplane structure has little or no effect on the behavior of the landing gear. Also, load time histories obtained on a rigid-body basis are often used as the forcing function in a dynamic analysis to determine the inertia loads and stresses in flexible airplane structures, again under the assumption that the behavior of the landing gear is independent of the effects of airplane flexibility. Although it has been recognized that this assumption is not altogether valid, the errors involved have not been considered particularly significant in the past because: (a) The errors were thought to be on the conservative side and (b) until comparatively recently main landing gears have generally been located very close to the nodes of the fundamental bending mode of the wing, and the airplane therefore closely approximated a rigid body insofar as the behavior of the landing gear is concerned. However, the trend toward increased size of airplanes, the disposition of large concentrated masses in outboard locations in the wings, the use of thinner wings, and the development of unconventional configurations tend to increase the flexibility of the airplane structure and reduce the natural frequencies of vibration. These characteristics tend to cause an increase in the amplitudes of the oscillatory motions of the landing-gear attachment points relative to the center of gravity of the flexible system during impact so that the effects of interaction are increased, both with regard to the behavior of the landing gear and the dynamic loads in the structure, particularly when the natural period of the fundamental mode of the structure approaches the time duration of the impact pulse.

A number of analytical studies and some simplified model tests (refs. 1 to 5) which have been made to evaluate the effects of structural flexibility on landing-gear loads have indicated some reduction in landing-gear force due to the effects of structural deformation. However, in view of the fact that these previous investigations considered only rather highly idealized linear-spring landing gears with either no damping at all or viscous damping, a further study of the effects of interaction between the landing gear and the airplane structure has been made with a more realistic representation of the landing gear. In the present analysis, as in reference 6, the landing gear is considered to have velocity-squared damping, polytropic air-compression springing, and exponential tire force-deflection characteristics, as is the case with conventional oleo-pneumatic landing gears in current use. The particular purposes of this investigation are to evaluate the effects of interaction on landing-gear behavior and to study the errors introduced into the calculated loads in the structure (applied loads, accelerations, bending moments, and shears) when a dynamic analysis is made on the basis of

applying the landing-gear forcing function for a rigid body to a flexible airplane. For these purposes, case-history studies, based on the structural properties of two large airplanes having considerably different mass and flexibility characteristics, are presented. In order to cover a range of parameters, the landing gear of each airplane was assumed to be located at three arbitrary spanwise positions in addition to its original location.

The basic analysis of the landing gear and the airplane structure as a coupled system is presented in a general form. In the numerical examples presented, however, the system is simplified by considering the motions of the airplane in its first two structural modes only. With these restrictions, the combination of airplane and landing gear can also be represented by an equivalent three-mass system which may be used in jig drop tests of landing gears to simulate the primary effects of structural flexibility. A similar type of concentrated-mass system was used in the study of the hydrodynamic impact of a flexible seaplane in reference 7.

SYMBOLS

General

g	gravitational constant
t	time after initial contact
τ	time variable of integration
T	time to maximum landing-gear force
t'	time after maximum landing-gear force
V_{V_o}	vertical velocity at initial contact
Ω	circular frequency of sine pulse
Ω_1	circular frequency of cosine pulse
λ	any variable
λ_p	value of any variable λ at end of pth interval subsequent to beginning of numerical-integration procedure

Landing Gear

A_a	pneumatic area of shock strut
A_h	hydraulic area of shock strut, $A_l - A_p$
A_l	internal cross-sectional area of shock-strut inner cylinder
A_n	net orifice area of shock strut, $A_o - A_p$
A_o	area of fixed opening in orifice plate
A_p	cross-sectional area of metering pin or rod in plane of orifice
C_d	orifice discharge coefficient
F_{V_s}	vertical component of force in shock strut subsequent to beginning of shock-strut deflection
$F_{V_g}(z_u)$	vertical force applied to tire at ground
m_u	unsprung mass below shock strut
m,r,m'	constants in tire force-deflection relationship
n	polytropic exponent for air-compression process in shock strut
p_{a_o}	air pressure in shock strut when fully extended
ρ	mass density of hydraulic fluid
v_o	air volume of shock strut when fully extended
s	shock-strut stroke
t_i	duration of impact pulse
θ	angle between shock-strut axis and vertical
W_u	weight of unsprung mass below shock strut
z_f	vertical displacement of landing-gear attachment point from position at initial contact

z_u vertical displacement of axle from position at initial contact

Distributed Structure

a_n generalized coordinate for nth mode

φ angle of twist of transverse station

φ_n modal function for torsion in nth mode

w vertical displacement of elastic axis from position at initial contact

w_n modal function of elastic axis for bending in nth mode

ζ vertical displacement of station mass centers from position at initial contact

ζ_n modal function of station mass centers for coupled bending-torsion in nth mode

ξ_n modal amplitude of landing-gear attachment point for coupled bending-torsion in nth mode

ϵ chordwise distance between elastic axis and station mass center

b wing span

BM bending moment

F vertical component of applied landing-gear force

f_1 natural frequency of first deflection mode

I_o polar moment of inertia of wing cross section about station mass center

I_{ea} polar moment of inertia of wing cross section about elastic axis

K radius of gyration of wing station about elastic axis

L lift force per unit length of span

m mass per unit length of span

M_n	generalized mass for nth mode
ω_n	circular frequency of nth mode
Q_n	generalized force in nth mode
S	shear
t_n	natural period of nth mode
x	chordwise distance between elastic axis and any arbitrary point
x_f	chordwise distance between elastic axis and landing-gear attachment point
y	spanwise distance from airplane center plane to any transverse station
y_g	spanwise distance from airplane center plane to landing-gear station
z	vertical displacement of any point from position at initial contact
z_f	vertical displacement of landing-gear attachment point from position at initial contact
z_u	vertical displacement of axle from position at initial contact
δa_n	virtual displacement of generalized coordinate of nth mode
δW_n	virtual work in nth mode

Equivalent Three-Mass System

a_0	vertical displacement of center of gravity of spring-connected masses from position of initial contact
k	spring constant
L_f	lift force acting on mass m_f
L_s	lift force acting on mass m_s

m_f	mass acting directly on landing gear
m_s	elastically supported mass
ω_1	natural frequency of vibration of spring-connected masses
u	deflection of spring
W_f	weight of mass acting directly on landing gear
W_s	weight of elastically supported mass
z_f	vertical deflection of landing-gear attachment point
z_s	vertical deflection of elastically supported mass
z_u	vertical displacement of axle from position at initial contact

Aerodynamic

A	total wing area
A_i	wing area assumed concentrated at station i
C_L	lift coefficient
C_{L_o}	lift coefficient at instant of initial contact
C_{L_α}	lift-curve slope
γ	flight-path angle
γ_o	flight-path angle at instant of initial contact
ρ	mass density of air
V_L	landing speed of airplane
W	total weight of airplane

Subscripts:

a	aerodynamic
f	landing-gear attachment point
g	landing-gear station
i	any spanwise station
n	pertaining to the nth mode
0	zero or rigid-body mode
τ	at instant of initial shock-strut motion
T	at instant of maximum landing-gear force
max	maximum

The use of dots over symbols indicates differentiation with respect to time t or τ. All translations are positive downward (see figs. 1 to 3). The absolute value of any term is indicated by $|()|$.

ANALYSIS

In order to study the behavior of a landing gear and a flexible airplane structure as mutually interacting elements of a coupled system, the equations for the landing-gear force are combined with the equations of motion of the structure. The motions of the structure are treated by the mode-superposition approach, wherein the deflections of the structure are expanded in terms of its natural modes of vibration. The effects of interaction between the landing gear and the structure are introduced by expressing the landing-gear force in terms of the motions of the landing-gear attachment point and the wheel axle (or unsprung mass) rather than as an arbitrary function of time.

Because conventional oleo-pneumatic shock struts do not begin to deflect until some finite time after initial contact of the tire with the ground, the impact is treated in two parts, namely, the phases prior to and subsequent to the beginning of shock-strut deflection, where the initial conditions for the second phase are determined from the terminal conditions for the first phase.

In the first part of the analysis, the equations for the landing-gear force are presented. Then, the deflections of the structure are expanded in terms of coupled modes and the resulting equations of motion

for the system are presented in a general form. For the purpose of indicating the effects of interaction, however, the system used in the numerical trend studies has been simplified by restricting consideration of the structural deflections to the first two modes of the expansion. Within the framework of this two-mode treatment, it is also shown that the airplane structure can be represented by an equivalent system of spring-connected concentrated masses, which may be used to simulate the effects of structural flexibility in jig drop tests of landing gears.

Landing-Gear Force

An analysis of the behavior of the conventional type of oleo-pneumatic landing gear was presented in reference 6. In this study the mass above the landing gear was considered as a rigid body; the system treated therefore had two degrees of freedom and is schematically represented in figure 1. The analysis of the landing gear considered the velocity-squared damping of the metering orifice, the air-compression springing of the shock strut, the nonlinear force-deflection characteristics of the tire, and the internal shock-strut friction forces. Calculated time histories of the landing-gear forces and the motions of the system were in good agreement with experimental data obtained in drop tests.

In the present study the rigid mass is replaced by a flexible airplane structure, but the treatment of the landing gear is essentially the same as that in reference 6. However, since conventional landing gears are inclined forward so as to minimize normal forces and bending moments due to the combination of vertical and drag forces, it will be assumed that the resultant force on the landing gear lies along the axis of the shock strut so that bending moments and resulting internal friction forces are neglected in the present analysis.

In view of the fact that conventional oleo-pneumatic shock struts are preloaded with air and therefore do not begin to deflect until some finite time t_τ after initial contact of the tire with the ground, the impact must be treated in two phases. In the first phase, since the strut is effectively rigid, the landing gear has only one degree of freedom and the motion of the complete system of the landing gear and airplane is governed by the force between the tire and the ground. This ground force arises from the deflection of the tire and, in general, may be written as

$$F_{V_g} = F_{V_g}(z_u) \tag{1}$$

the exact variation depending on the tire force-deflection characteristics. Prior to the beginning of shock-strut deflection

$$F_{V_g} = F_{V_g}(z_f) \qquad (t \leqq t_\tau) \tag{1a}$$

since $z_u = z_f$. (This relationship is exact when the landing gear is vertical and holds very closely when the gear is inclined.)

The shock strut starts to deflect at the time t_τ when the force exerted on the airplane by the shock strut becomes equal to the air-pressure preloading force in the strut. At this instant the free-body equation for the unsprung mass of the landing gear is

$$m_u \ddot{z}_{f_\tau} + F_{V_g}\left(z_{f_\tau}\right) = p_{a_o} A_a \cos\theta + W_u \qquad (t = t_\tau) \tag{2}$$

Equation (2) provides the relationship between the terminal conditions for the first phase of the impact which, in conjunction with the solution of the equations of motion for the complete system prior to shock-strut deflection, determines the time t_τ when the shock-strut begins to deflect and, thus, the terminal values of the variables for the first phase of the impact, which also serve as the initial conditions for the second phase of the impact.

After the shock strut begins to deflect, the landing gear has two degrees of freedom since the motions of the landing-gear attachment point and the motions of the unsprung mass are no longer the same. The equation for the vertical component of the force transmitted to the airplane by the landing gear after the shock strut starts to deflect is (see ref. 6)

$$F_{V_s} = \left[\frac{\dot{s}}{|\dot{s}|}\frac{\rho A_h{}^3}{2\left(C_d A_n\right)^2}\dot{s}^2 + p_{a_o} A_a \left(\frac{v_o}{v_o - A_a s}\right)^n\right]\cos\theta \qquad (t \geqq t_\tau) \tag{3}$$

where

$$s = \frac{z_f - z_u}{\cos\theta}$$

$$\dot{s} = \frac{\dot{z}_f - \dot{z}_u}{\cos\theta}$$

The equation of motion of the unsprung mass is

$$m_u\ddot{z}_u + F_{V_g}(z_u) = F_{V_s} + W_u \qquad (t \geqq t_\tau) \tag{4}$$

In equation (3) the first term represents the hydraulic force in the shock strut, where the factor $\dot{s}/|\dot{s}|$ indicates the change in sign required between the compression and extension strokes. (During the extension stroke of the shock strut, because of the action of the rebound check valve or "snubber" incorporated in most landing gears, the net orifice area A_n will generally be smaller and the orifice discharge coefficient C_d will be different from the values which apply during the compression stroke.) The second term of equation (3) expresses the air-compression force in the strut, based on a polytropic pressure-volume relationship. In equation (4), the force arising from the deflection of the tire may be expressed as $F_{V_g}(z_u) = mz_u^r$ for the usual type of pneumatic tire, where m and r are constants for each regime of the tire-deflection process (see ref. 6).

Equations of Motion of the Airplane

Differential equations of airplane structure.- In the mode-superposition approach, the structure is considered to deflect in its natural modes of vibration and the total displacement of any point in the system is the sum of the displacements of the point in all the modes considered. With this approach the motions are separated into functions which depend only on the space coordinates and functions which depend on the time variable.

In the case of a landing impact the process is discontinuous at the instant t_τ when the shock strut begins to deflect. In the first phase of the impact the shock strut is effectively rigid so that the motion of the unsprung mass of the landing gear is essentially the same as the motion of the landing-gear attachment point and the force transmitted by the landing gear to the airplane is the algebraic sum of the ground force due to tire deflection, the inertia reaction of the unsprung mass, and the weight of the unsprung mass. In the second phase of the impact, the motion of the unsprung mass is not the same as the motion of the landing-gear attachment point and the force applied to the airplane is governed by the relative motion between the landing-gear attachment point and the unsprung mass, as given by equation (3).

The notation employed in the analysis is indicated in figure 2. A typical transverse station located at a spanwise distance y from the airplane center plane is considered. The mass per unit length of span

is designated by m. The translation of the elastic axis at the station is denoted by w; ζ is the translation of the station mass center; ϵ is the chordwise distance between the station mass center and the elastic axis; and φ is the angle of twist of the station. The translation of an arbitrary point located at a chordwise distance x from the elastic axis is designated by z. The spanwise distance from the center plane of the airplane to the landing-gear station is indicated by y_g. The translation of the landing-gear attachment point, or force-application point, is designated z_f; the distance between the landing-gear attachment point and the elastic axis is denoted by x_f.

In the most general case, the expansion of the deflection of the structure in terms of its natural coupled modes of vibration may be written as

$$w(y,t) = \sum_{n=0}^{\infty} a_n(t) w_n(y) \tag{5}$$

and

$$\varphi(y,t) = \sum_{n=0}^{\infty} a_n(t) \varphi_n(y) \tag{6}$$

where the subscript n denotes the order of any mode, a_n is the generalized coordinate in the nth mode, and w_n and φ_n are the corresponding modal functions for bending and torsion, respectively.[1]

For later use it is convenient to introduce expressions for the displacements at other points in the structure. Since the translation of the station mass centers is given by $\zeta = w + \epsilon\varphi$,

$$\zeta(\epsilon,y,t) = \sum_{n=0}^{\infty} a_n(t) \zeta_n(y) \tag{7}$$

where the modal function $\zeta_n = w_n + \epsilon\varphi_n$. The translation of any arbitrary point along the chord is given by $z = w + x\varphi$; therefore,

$$z(x,y,t) = \sum_{n=0}^{\infty} a_n(t) z_n(y) \tag{8}$$

---

[1]The zero mode represents the translation of the airplane as a rigid body; therefore, $w_0 = 1$. In the present analysis, rigid-body pitching is neglected; therefore $\varphi_0 = 0$.

where the modal function $z_n = w_n + x\varphi_n$. The translation of the landing-gear attachment point is given by $z_f = w + x_f\varphi$; therefore,

$$z_f(x_f,y_g,t) = \sum_{n=0}^{\infty} a_n(t)\xi_n(y_g) \tag{9}$$

where the modal function $\xi_n = w_n + x_f\varphi_n$.

By application of Lagrange's equation and the orthogonality relationships between coupled modes, it can be shown (see, for example, refs. 8 to 10) that the equation of motion for the airplane in the nth mode may be written as

$$M_n\ddot{a}_n + M_n\omega_n a_n = Q_n \qquad (n = 0,1,2, \ldots) \tag{10}$$

where M_n is termed the generalized mass for the nth mode and Q_n is the generalized force, as determined from virtual-work considerations. For a continuous system,

$$\left.\begin{aligned} M_n &= \int_0^{b/2} mw_n^2 dy + 2\int_0^{b/2} m\epsilon\varphi_n w_n\, dy + \int_0^{b/2} mK^2\varphi_n^2 dy \\ &= \int_0^{b/2} m\zeta_n^2 dy + \int_0^{b/2} I_o\varphi_n^2 dy \end{aligned}\right\} \tag{11}$$

In practice the spanwise mass distribution is often approximated by breaking up the distribution into discrete masses which are concentrated at a finite number of stations along the span. With this approach equation (11) may be written as

$$\left.\begin{aligned} M_n &\approx \sum_i \left(m_i w_{n_i}^2 + 2m_i\epsilon_i\varphi_{n_i}w_{n_i} + m_i K_i^2\varphi_{n_i}^2\right) \\ &\approx \sum_i \left(m_i\zeta_{n_i}^2 + I_{o_i}\varphi_{n_i}^2\right) \end{aligned}\right\} \tag{11a}$$

where the subscript i denotes any spanwise station.

For the rigid-body mode $(n = 0)$, since $w_0 = \zeta_0 = 1$ and $\varphi_0 = 0$,

$$M_0 = \int_0^{b/2} m\,dy \approx \sum_i m_i$$

The relationship between Q_n and the external forces can be determined by application of virtual-work principles. By definition, the work done in the nth mode by the generalized force acting through a virtual displacement of the generalized coordinate of the mode is equal to the work done by the external forces acting through virtual displacement of their points of application in the mode. Thus, the virtual work done by the generalized force in the nth mode is

$$\delta W_n = Q_n\,\delta a_n \tag{12}$$

In the case of an airplane during landing the external forces are the distributed lift forces $L(y)$, the distributed weights $gm(y)$, and the force F transmitted by the landing gear. The virtual work done by these external forces in the nth mode is therefore given by

$$\delta W_n = -\left[\int_0^{b/2} L\delta a_n z_n\,dy - g\int_0^{b/2} m\delta a_n \zeta_n\,dy + F\delta a_n \xi_n\right]$$

$$= -\delta a_n\left(\int_0^{b/2} Lz_n\,dy - g\int_0^{b/2} m\zeta_n\,dy + F\xi_n\right) \tag{13}$$

Equating equations (12) and (13) gives the following relationship for Q_n:

$$Q_n = -\left(\int_0^{b/2} Lz_n\,dy - g\int_0^{b/2} m\zeta_n\,dy + F\xi_n\right)$$

Therefore, the equation of motion of the structure in the nth mode is

$$M_n\ddot{a}_n + M_n\omega_n^2 a_n = -F\xi_n - \int_0^{b/2} Lz_n\,dy - g\int_0^{b/2} m\zeta_n\,dy$$

$$(n = 0,1,2, \ldots) \tag{14}$$

For the rigid-body mode $(n = 0)$, since $\omega_0 = 0$ and $z_0 = \zeta_0 = \xi_0 = 1$, equation (14) becomes

$$M_0\ddot{a}_0 = - F - \int_0^{b/2} (L - gm)dy$$

subject to the initial conditions

$$a_0(0) = 0$$

and

$$\dot{a}_0(0) = V_{V_0}$$

If the airplane is assumed to be free of oscillations at the time of initial contact,

$$\dot{a}_n(0) = \ddot{a}_n(0) = 0 \qquad (n \neq 0)$$

Since

$$F(0) = - W_u$$

equation (14) applied to the instant $t = 0$ gives

$$a_n(0) = \frac{1}{M_n\omega_n^2}\left(W_u\xi_n - \int_0^{b/2} Lz_n\, dy + g\int_0^{b/2} m\zeta_n\, dy\right) \qquad (n \neq 0)$$

This relationship indicates that, in general, a finite static deflection in the flexible modes will be present at the time of initial contact. At any subsequent time the deflection will be equal to this initial static deflection plus an additional deflection a_{n_t} which varies with time; that is, $a_n = a_n(0) + a_{n_t}$. This substitution permits equation (14) to be written as

$$M_n\ddot{a}_{n_t} + M_n\omega_n^2 a_{n_t} = -(F + W_u)\xi_n \qquad (n \neq 0) \qquad (15)$$

subject to the initial conditions

$$a_{n_t}(0) = \dot{a}_{n_t}(0) = 0$$

In the remainder of the paper, for the sake of simplicity of notation, the subscript t will be dropped, with the understanding that a_n represents the time-varying part of the displacement of the nth mode, so that equation (15) is written as

$$M_n\ddot{a}_n + M_n\omega_n^2 a_n = -(F + W_u)\xi_n \qquad (n \neq 0) \qquad (15a)$$

If the external forces are specified solely as functions of time, the equations of motion for each mode of the system are uncoupled and can be solved individually. However, when the external forces depend on the motions of the system, as in the case of the landing-gear force during a landing impact, the relationships between the external forces and the motions in the modes serve to couple the equations of motion so that they must be solved simultaneously. Furthermore, in the case of landing impact, since the process has two phases, as previously discussed, the equations of motion for each phase must be solved separately, where the initial conditions for the second phase are the same as the terminal conditions for the first phase.

Motion prior to beginning of shock-strut deflection.- Since the shock strut is effectively rigid in the first phase of the impact, the force transmitted by the landing gear to the airplane, F in equation (15a), is equal to the ground force $F_{V_g}(z_f)$ less the inertia reaction of the unsprung mass and the weight of the unsprung mass, as may be seen by considering the unsprung mass as a free body; thus,

$$F_{t \leq t_\tau} = F_{V_g}(z_f) + m_u\ddot{z}_f - W_u$$

so that the motions of the system during the first phase of the impact are governed by the following set of differential equations:

$$\left.\begin{aligned} M_0\ddot{a}_0 &= -\left[F_{V_g}(z_f) + m_u\ddot{z}_f - W_u\right] - Z_0 \\ M_1\ddot{a}_1 + M_1\omega_1{}^2a_1 &= -\left[F_{V_g}(z_f) + m_u\ddot{z}_f\right]\xi_1 \\ &\cdot \quad \cdot \quad \cdot \quad \cdot \quad \cdot \\ M_m\ddot{a}_m + M_m\omega_m{}^2a_m &= -\left[F_{V_g}(z_f) + m_u\ddot{z}_f\right]\xi_m \end{aligned}\right\} \qquad (t \leqq t_\tau) \qquad (16)$$

where

$$z_f = \sum_{n=0}^{m} a_n\xi_n$$

$$Z_0 = \int_0^{b/2} (L - gm)dy = \int_0^{b/2} L\,dy - M_0g$$

and the mth mode is the highest mode considered.

The initial conditions for equations (16) are the conditions at the instant of initial contact, namely,

$$a_0(0) = 0$$

$$\dot{a}_0(0) = V_{V_0}$$

and

$$a_n(0) = \dot{a}_n(0) = 0 \qquad (n \neq 0)$$

As previously indicated, the first phase of the impact terminates at the time t_τ when the force in the shock strut becomes equal to the air-pressure preload force. The terminal conditions at this instant, as determined by consideration of the unsprung mass as a free body, are given by equation (2), namely,

$$m_u\ddot{z}_{f_\tau} + F_{V_g}\left(z_{f_\tau}\right) = p_{a_0}A_a \cos\theta + W_u$$

The solution of equations (16) in conjunction with equation (2) permits the determination of the time t_T when the shock strut begins to deflect and the values of the motion variables at this instant; these values then serve as the initial conditions for the second phase of the impact.

Motion subsequent to beginning of shock-strut deflection.- In the second phase of the impact the force transmitted by the landing gear, F in equation (15a), is the vertical component of the shock-strut force F_{V_s}, as given by equation (3). Thus, the motions of the system during the second phase of the impact are governed by the following set of differential equations:

$$\left.\begin{aligned} M_0\ddot{a}_0 &= -\left(F_{V_s} + Z_0\right) \\ M_1\ddot{a}_1 + M_1\omega_1^2 a_1 &= -\left(F_{V_s} + W_u\right)\xi_1 \\ &\cdot \quad \cdot \quad \cdot \quad \cdot \quad \cdot \\ M_m\ddot{a}_m + M_m\omega_m^2 a_m &= -\left(F_{V_s} + W_u\right)\xi_m \\ m_u\ddot{z}_u + F_{V_g}(z_u) &= F_{V_s} + W_u \end{aligned}\right\} \qquad (t > t_T) \qquad (17)$$

where

$$F_{V_s} = F_{V_s}(z_f - z_u,\ \dot{z}_f - \dot{z}_u)$$

as given by equation (3); and

$$z_f = \sum_{n=0}^{m} a_n \xi_n$$

The first m equations of equations (17) represent the motions of the airplane structure in its first m modes, whereas the last equation of the set is the equation of motion of the unsprung mass of the landing gear as previously given by equation (4). The initial conditions for equations (17) are the terminal conditions for equations (16) as previously discussed. In view of the fact that the landing-gear forcing

term F_{V_s} is highly nonlinear, analytical solution of the system of equations (17) does not appear possible so that it is necessary to resort to numerical-integration or analog methods.

Simplified System Considered in Numerical Studies

The preceding section has presented the equations of motion for a flexible airplane coupled to a landing gear, which permit calculation of the motions of the system during a landing impact with consideration of as many modes as may be desired. For the study of the effects of interaction between the landing gear and the structure, however, it appears that the primary effects of structural flexibility on the behavior of the landing gear can be represented by considering only the first deflection mode in addition to the rigid-body mode.[2] This simplification, which greatly reduces the amount of computational work, is felt to be justified for the purposes of the present investigation since both theoretical considerations and experimental data indicate that the higher modes should have relatively little effect on the landing-gear performance. With this assumption the equations of motion reduce to

$$\left.\begin{aligned} M_0\ddot{a}_0 &= -\left[F_{V_g}(z_f) + m_u\ddot{z}_f - W_u\right] - Z_0 \qquad (18a)\\ M_1\ddot{a}_1 + M_1\omega_1^2 a_1 &= -\left[F_{V_g}(z_f) + m_u\ddot{z}_f\right]\xi_1 \qquad (18b)\end{aligned}\right\} \quad (t \leq t_T)$$

and

$$\left.\begin{aligned} M_0\ddot{a}_0 &= -\left(F_{V_s} + Z_0\right) \qquad (19a)\\ M_1\ddot{a}_1 + M_1\omega_1^2 a_1 &= -\left(F_{V_s} + W_u\right)\xi_1 \qquad (19b)\\ m_u\ddot{z}_u + F_{V_g}(z_u) &= F_{V_s} + W_u \qquad (19c)\end{aligned}\right\} \quad (t > t_T)$$

[2]In a dynamic analysis, stresses in the structure due to excitation of the higher modes can be approximated by calculating the response of such modes, individually, to the forcing function determined for the landing gear coupled with the rigid-body and first deflection modes. This procedure should be a considerable improvement over the use of the rigid-body forcing function as a basis for response calculations in cases where the landing-gear attachment points experience appreciable deflections relative to the mass center of the system.

where

$$z_f = a_0 + a_1\xi_1$$

and

$$m_u\ddot{z}_{f_\tau} + FV_g\left(z_{f_\tau}\right) = pa_o \cos\theta + W_u \qquad (t = t_\tau)$$

The solution of equations (18) and the determination of the conditions at the time t_τ when the shock strut begins to deflect, which serve as the initial conditions for equations (19), are treated in appendix A. With these initial conditions, equations (19) may be solved by numerical integration or analog methods.

From the time-history solutions for the motions of the system thus obtained, the accelerations and inertia loads at any point in the structure can be calculated from the equations presented in appendix B.

Equivalent Three-Mass System

It is of interest to note that the equations of motion previously presented not only represent the distributed system of the airplane but can also be used to define equivalent systems of spring-connected masses, where the number of masses above the landing gear is equal to the number of modes considered. For the particular case where two modes are considered the equivalent system is one containing three masses, one of which is the unsprung mass of the landing gear. The use of such a three-mass system provides a relatively simple means for simulating the primary effects of structural flexibility in actual drop tests of landing gears in a drop-test jig.

In the equivalent three-mass system (see fig. 3), m_f represents the mass to which the landing gear is directly attached and m_s is the elastically connected mass. The displacement of m_f relative to its position at the instant of initial contact is denoted by z_f; the displacement of m_s is designated z_s, whereas the displacement of the axle or unsprung mass m_u is z_u. The spring constant of the elastic member is denoted by k. Separate lift forces L_s and L_f will be considered to act on the masses m_s and m_f.

In order that the three-mass system represents the airplane properly, z_f, z_u, m_u, and, of course, the landing-gear characteristics must be the

same for the two systems so that the landing-gear force is the same; and m_f, m_s, k, and the applied lift forces must be determined from the relationships between the equations of motion for the three-mass system and the equations of motion for the airplane.

Consideration of the forces acting on each mass as a free body (see fig. 3) leads to the following equations of motion for the three-mass system:

Prior to beginning of shock-strut deflection:

$$\left.\begin{aligned} (m_f + m_u)\ddot{z}_f - k(z_s - z_f) + L_f - (W_f + W_u) &= -F_{V_g}(z_f) \qquad (20a)\\ m_s\ddot{z}_s + (m_f + m_u)\ddot{z}_f + (L_s + L_f) - (W_s + W_f + W_u) &= -F_{V_g}(z_f) \qquad (20b) \end{aligned}\right\} \quad (t \leq t_T)$$

where

$$m_u\ddot{z}_{f_T} + F_{V_g}\left(z_{f_T}\right) = p_{a_o}A_a \cos\theta + W_u \qquad (t = t_T)$$

Subsequent to beginning of shock-strut deflection:

$$\left.\begin{aligned} m_f\ddot{z}_f - k(z_s - z_f) + L_f - W_f &= -F_{V_s} \qquad (21a)\\ m_f\ddot{z}_f + m_s\ddot{z}_s + (L_s + L_f) - (W_s + W_f) &= -F_{V_s} \qquad (21b)\\ m_u\ddot{z}_u + F_{V_g}(z_u) &= F_{V_s} + W_u \qquad (21c) \end{aligned}\right\} \quad (t > t_T)$$

The problem is to determine the relationships between m_s, m_f, k, L_s, and L_f for the airplane so that equations (20) are equivalent to equations (18) and equations (21) are equivalent to equations (19) with the requirement that the motions of the landing gear in the three-mass system be the same as for the airplane, that is,

$$z_f = a_0 + a_1\xi_1$$

and that z_u be the same in both systems. Since equations (19c) and (21c) are identical, they need not be considered further in evaluating the unknown constants for the three-mass system.

It is apparent that equations (20a) and (20b) as well as equations (21a) and (21b) can be written as

$$m_f\ddot{z}_f - k(z_s - z_f) + L_f - W_f = -F \tag{22a}$$

$$m_f\ddot{z}_f + m_s\ddot{z}_s + (L_s + L_f) - (W_s + W_f) = -F \tag{22b}$$

where

$$F = F_{V_g}(z_u) + m_u\ddot{z}_u - W_u$$

and

$$z_u = z_f \qquad (t \leqq t_T)$$

$$z_u \neq z_f \qquad (t > t_T)$$

Similarly, equations (18a) and (18b) and equations (19a) and (19b) can be written as

$$M_0\ddot{a}_0 + Z_0 = -F \tag{23a}$$

$$\frac{M_1}{\xi_1}\ddot{a}_1 + \frac{M_1}{\xi_1}\omega_1^2 a_1 + W_u = -F \tag{23b}$$

Thus, the problem is reduced to determining the constants for the three-mass system so as to make equations (22) identically equivalent to equations (23). This may be done in any of several different ways. For example, since the structure is taken as linear, let

$$z_s = a_0 + a_1\beta$$

where β is a constant to be determined. Substituting for z_f and z_s in equations (22a) and (22b) and eliminating $\ddot{a}_0$ between these equations gives

$$m_f(\xi_1 - \beta)\ddot{a}_1 + \frac{k}{m_s}(\xi_1 - \beta)(m_f + m_s)a_1 + L_f - W_f + \frac{m_f}{m_s}(W_s - L_s) = -F \qquad (24)$$

whereas, subtracting equation (22a) from equation (22b), with the same substitutions, gives

$$\ddot{a}_0 + \beta\ddot{a}_1 + \frac{k}{m_s}(\beta - \xi_1)a_1 + \frac{L_s}{m_s} - g = 0 \qquad (25)$$

Equation (24) is directly comparable with equation (23b). Combining equations (23a) and (23b) so as to eliminate F and to make the coefficient of $\ddot{a}_0$ equal to unity gives the following equation with which equation (25) may be directly compared:

$$\ddot{a}_0 - \frac{M_1}{M_0\xi_1}\ddot{a}_1 - \frac{M_1\omega_1^2}{M_0\xi_1}a_1 + \frac{Z_0 - W_u}{M_0} = 0 \qquad (26)$$

In order to evaluate the constants for the three-mass system, each term in equations (24) and (25) is set equal to the corresponding term in equations (23b) and (26), respectively, the constants in each equation being considered as a single term. This procedure gives six simultaneous equations, the solution of which yields the following expressions for the constants in the three-mass system:

$$m_s + m_f = M_0 \qquad (27)$$

$$L_s + L_f = M_0 g + Z_0 \qquad (28)$$

$$m_s = \frac{M_0^2\xi_1^2}{M_1 + M_0\xi_1^2} \qquad (29)$$

$$m_f = \frac{M_1 M_0}{M_1 + M_0\xi_1^2} \qquad (30)$$

$$\frac{m_s}{m_f} = \frac{M_0\xi_1^2}{M_1} \tag{31}$$

$$k = M_1\omega_1^2\left(\frac{M_0\xi_1}{M_1 + M_0\xi_1^2}\right)^2 \tag{32}$$

$$L_s = \frac{M_0\xi_1^2(Z_0 - W_u)}{M_1 + M_0\xi_1^2} + W_s \tag{33}$$

and

$$L_f = \frac{M_1Z_0 + M_0W_u\xi_1^2}{M_1 + M_0\xi_1^2} + W_f \tag{34}$$

where

$$\beta = -\frac{M_1}{M_0\xi_1} \tag{35}$$

and

$$m_f\ddot{z}_f + m_s\ddot{z}_s = M_0\ddot{a}_0 \tag{36}$$

With the foregoing substitutions, equations (22) are identically equivalent to equations (23); thus, the three-mass system with the specified values of m_s, m_f, k, L_s, and L_f can be considered to be equivalent to the airplane in its first two modes during both the first and second stages of the impact. Equations (27) and (28) are required to satisfy the equations of motion for the airplane as a rigid body, whereas equations (29) to (34) are required for proper representation of the airplane in its first flexible mode. With this approach the structural properties of the airplane are defined by three parameters: the total mass above the landing gear M_0, the mass ratio m_s/m_f, and the natural frequency ω_1.

The solution of the equations of motion during the first phase of the impact and the determination of the conditions at the instant of initial shock-strut deflection t_τ are treated in appendix A. With these conditions as initial conditions, the equations of motion for the second phase of the impact can be solved by numerical-integration or analog methods. From the time-history solutions for the motion of the three-mass system, the inertia loads and bending moments at any point in the airplane structure can be calculated by use of the equations in appendix B.

Solution of Equations of Motion

In view of the fact that the equations of motion subsequent to time t_τ are highly nonlinear and therefore cannot be solved in closed form, it is necessary to resort to numerical-integration or analog methods. Various numerical-integration procedures are given in references 11 to 13. Appendix A of reference 6 illustrates the application of several such methods to the problem of the impact of a landing gear attached to a rigid mass. One of these methods, which may be termed the "quadratic procedure," was used to obtain those numerical results presented in this paper which could not be obtained analytically.

In this procedure, which involves a step-by-step solution of the equations of motion, the following difference equations (ref. 11, p. 16) based on a quadratic variation of displacement over successive finite time intervals are used to replace the derivatives in the equations of motion:

$$\dot{\lambda}_p = \frac{\lambda_{p+1} - \lambda_{p-1}}{2\,\Delta t}$$

and

$$\lambda_p = \frac{\lambda_{p+1} - 2\lambda_p + \lambda_{p-1}}{(\Delta t)^2}$$

where λ_p is the value of any variable at the end of the pth interval subsequent to the beginning of the process and Δt is the time interval. The difference equations of motion obtained by substituting these expressions into the differential equations of the system then become essentially extrapolation formulas which permit calculation of the displacements to come from the values of displacement already calculated, the whole procedure starting out with the initial conditions of the process. With

the displacement time histories thus calculated, the velocities and accelerations are then determined from the foregoing difference equations.

CALCULATED RESULTS AND DISCUSSION

Cases Considered

In order to investigate the effects of structural flexibility on the behavior of the landing gear and the loads in the airframe, several case-history studies are presented which cover a range of airplane mass ratios m_s/m_f. The calculations are based on the structural properties of two large airplanes having considerably different mass and flexibility characteristics. Airplane A is representative of a four-engine propeller-driven World War II bomber having a gross weight of 47,200 pounds and a natural frequency of vibration in the first coupled bending-torsion mode of 3.37 cycles per second. The structural characteristics used for airplane B are representative of a present-day swept-wing six-jet-engine bomber having a gross weight of 125,000 pounds and a natural frequency of 1.29 cycles per second in the first coupled bending-torsion mode. The landing-gear characteristics used for airplane A were based on the manufacturer's data, whereas, for airplane B because information was not available, the shock-strut characteristics were chosen so as to yield a landing gear which is essentially a scaled-up model of the landing gear of airplane A. The pertinent numerical data for airplanes A and B are given in tables I and II, respectively; the modal functions for the first coupled bending-torsion mode are plotted in figure 4.

The main landing gears of airplane A were located in the inboard engine nacelles very close to the nodes of the first coupled bending-torsion mode; in the case of airplane B the landing gear is of the bicycle type and is located in the airplane center plane. The position of the landing gear (since it determines the value of the modal amplitude ξ_1) in conjunction with the values of M_0 and M_1 governs the value of the mass ratio m_s/m_f for each case. (See eq. (31).)

In order to represent a broader range of mass and flexibility effects, the calculations for each airplane were made for four mass ratios corresponding to three arbitrary landing-gear positions in addition to the original landing-gear location. In practice, of course, a change in landing-gear location would probably necessitate a modification of the wing structure and result in some change in the modal characteristics and, thus, the mass ratio. The main purpose of the calculations, however, is to indicate the effect of mass ratio on the behavior of the system, and the exact locations of the landing gear which correspond to the mass ratios used are of secondary interest.

In the calculation of the mass ratio m_s/m_f, the landing-gear force was assumed to pass through the mass center of the landing-gear station. Since the modal characteristics used were for the complete airplane including the unsprung mass of the landing gear m_u, it was assumed that the unsprung mass was rigidly connected to the mass m_f in the equivalent three-mass system, as in the first phase of the impact, so that

$$\frac{m_s}{m_f + m_u} = \frac{M_0 \zeta_1^2}{M_1}$$

where M_0, M_1, and ζ_1 include the effects of the unsprung mass as part of the airplane mass distribution. The mass ratios considered and the corresponding landing-gear locations are as follows:

Airplane A		Airplane B	
Landing-gear location at -	Mass ratio, m_s/m_f	Landing-gear location at -	Mass ratio, m_s/m_f
Station 0	0.24	Station 0	0.22
Nodes	0	Nodes	0
Station 245	.52	Station 420	.85
Station 307	3.33	Station 504	2.84

When the landing gear is located at the node of the first flexible mode, this mode, of course, is not excited and, since higher modes are not considered in the numerical calculations, the airplane behaves as though it were a rigid body, its motion being governed by equation (23a). As might be expected, the farther away the landing gear is from the nodes, the larger is the effective flexibility of the system and, thus, the mass ratio.

In the calculation of the time histories of the motions of the system, the lift force was assumed to be constant during the impact and equal to the total weight of the airplane, that is,

$$\int_0^{b/2} L \, dy = M_0 g + W_u$$

so that

$$Z_0 = W_u$$

This assumption corresponds to the condition that

$$L_s = W_s$$

and

$$L_f = W_f + W_u$$

in the equivalent three-mass system.

On the basis of the calculations in reference 6, the shock-strut orifice discharge coefficient C_d was assumed as 0.9 and the polytropic exponent n for the air-compression process was taken as 1.12.

Effect of Interaction on Behavior of System

Time-history solutions for the motions of the system during impact at an initial vertical velocity of 10 feet per second have been made for the eight configurations previously mentioned. Figures 5 to 8 show the variation during impact of the more important quantities, such as the landing-gear force F, the responses $\ddot{a}_0/g$, $\ddot{a}_1/g$, $\ddot{z}_f/g$, $\ddot{z}_s/g$, the landing-gear-motion variables, and the accelerations at the mass centers of several stations along the span. Comparison of the calculated results for the flexible cases with those for the airplane as a rigid body (or landing gear at nodes, $m_s/m_f = 0$) indicates that the interaction between the flexible structure and the landing gear can result in an appreciable reduction in the applied landing-gear force (and thus, the nodal acceleration), the largest reductions occurring at the highest mass ratios. Furthermore, the reductions in landing-gear force at the higher mass ratios are greater for airplane B, because of its lower natural frequency, than for airplane A.

Consideration of the calculated time histories of the motion of the landing gear indicates how the interaction between the flexible structure and the landing gear affects the loads produced in the landing gear. Because of the flexibility of the structure, the landing-gear attachment point deflects upward relative to the nodes, or instantaneous center of mass of the system, as the applied force builds up and the deceleration

of the landing-gear attachment point is greater than in the case of the rigid airplane. Thus, the downward velocity of the shock-strut outer cylinder is more rapidly dissipated and the displacement of the outer cylinder is smaller throughout most of the impact. The tire deflection is also smaller; however, because of the high stiffness of the tire, the decrease in tire deflection is smaller than the decrease in outer-cylinder displacement. The net result is a reduction in strut stroke during that part of the impact when the maximum force occurs and an accompanying reduction in the strut telescoping velocity. Since the maximum landing-gear force is primarily due to the hydraulic resistance in the strut, because the strut stroke, and thus the air-compression force, is generally small at the time of maximum telescoping velocity, the decrease in telescoping velocity results in a decrease in shock-strut force.

In the case of airplane A with landing gear at station 307, the effect of interaction is a marked change in the shape, as well as in the magnitude, of the time histories. Because of the superimposed vibrations of the structure, the shock-strut telescoping velocity (see fig. 5) has acquired an oscillatory character with two peaks of the same amplitude. However, since the second telescoping-velocity peak occurs when the stroke is large, the superposition of the high air-compression force on the hydraulic-force results in a total-force time history the second peak of which is much higher than the first (see F-t curves, fig. 5) and which is also higher than might be expected from the results for the smaller mass ratios, which have a considerably different appearance. In the case of airplane B, because of the lower natural frequency, this double-peaked characteristic does not appear even for the largest mass ratio, all mass ratios yielding time histories similar in shape, the maximum force decreasing in a regular manner with increasing mass ratio.

The extent to which the first flexible modes of airplanes A and B are excited by the impacts may be observed by examining the time histories of a_1, $\dot{a}_1$, and $\ddot{a}_1$. As may be expected, the higher the mass ratio, the greater is the degree of excitation.

From the calculated values of $\ddot{a}_0/g$ and $\ddot{a}_1/g$ or $\ddot{z}_f/g$ and $\ddot{z}_s/g$, the acceleration at any point along the span may be computed by means of the equations in appendix B. Figures 6 and 8 show time histories of the acceleration at the mass centers of several stations for each of the landing-gear locations considered. Because of the combined effects of the changes in the landing-gear forcing function and in the degree of excitation of the flexible modes, a given change in landing-gear location may result in an increase in acceleration at some stations and a reduction in acceleration at other stations.

Figures 5 and 7 also show time histories of the acceleration $\ddot{z}_s/g$ which would be experienced by the elastically connected mass m_s in the

equivalent three-mass system, as in a drop test. The reduction in acceleration with increasing mass ratio is evident. As previously indicated, if such a drop test were made, the measured accelerations $\ddot{z}_f/g$ and $\ddot{z}_s/g$ could be used to calculate the accelerations and stresses that would result at any point in the corresponding airplane structure by means of the equations presented in appendix B.

Figure 9(a) presents a summary graph showing the effects of structural flexibility and interaction on the maximum landing-gear force for the various configurations considered. As previously indicated, the reductions in landing-gear force are greater for airplane B than for airplane A because of the lower natural frequency of the former airplane. For the range of mass ratios representative of existing and proposed large airplanes, for example, values up to about 0.5, reductions in landing-gear force up to between 15 and 20 percent may be possible. Along the same lines, figure 9(b) shows the effects of interaction on the acceleration response of the landing-gear attachment point and on the acceleration of the elastically connected mass in the equivalent three-mass system.

Effects of Neglecting Interaction in the Calculation of Dynamic Loads

In the usual procedures of dynamic analysis of landing loads it is customary to neglect the effects of interaction on the landing-gear forcing function and to determine the dynamic loads in the structure by calculating the response of the structure to the forcing function which would be obtained if the airplane were a rigid body, this rigid-body forcing function being either calculated or, more frequently, determined on the basis of drop tests of the landing gear with a rigid mass. In practice, either the actual rigid-body forcing function or some simplified analytical approximation of it (see, for example, fig. 10) is used.

In order to evaluate the errors introduced by neglect of interaction effects, the root bending moments and shears determined from the interaction solutions for airplanes A and B are compared in figures 11 and 12 with those determined by calculating the response of the various configurations to the rigid-body forcing functions previously presented and to simple analytical approximations to the rigid-body forcing functions. These bending moments and shears are total values due to both inertia and aerodynamic forces, the latter being included to permit comparison with the steady-flight values. For reference purposes, figures 11 and 12 also show the root bending moments and shears which would be experienced by a completely rigid airplane.

The calculation of the response of systems with two degrees of freedom to predescribed forcing functions is treated in appendix C. The

response of the various configurations to the rigid-body forcing function was calculated by application of the numerical-integration procedure previously described, whereas the response to the analytical forcing functions was obtained in closed form. The rigid-body forcing functions for airplanes A and B and their approximations are shown in figure 10. In the case of airplane A, the rigid-body forcing function was approximated by a pulse composed of sine and cosine segments; for airplane B, a simple sine pulse was used. The equations for calculating the inertia moments and shears from the response of the system are given in appendix C; simplified expressions for calculating the moments and shears due to the aerodynamic forces are given in appendix D.

From figures 11 and 12 it can be seen that the bending moments and shears calculated from the response to the rigid-body forcing function are larger than those determined from the interaction solutions, the differences being greater for the higher mass ratios where the effects of interaction result in a greater reduction in the magnitude of the landing-gear forcing function. From these particular examples, it appears that neglect of the effects of interaction on the landing-gear forcing function can lead to overconservatism in design not only of the landing gear but also of the structure, particularly for very flexible configurations with high mass ratios. As might be expected, there was relatively little difference in the loads calculated from the response to the analytical approximations and from the response to the rigid-body forcing function.

It is of interest to note that in the case of airplane A the loads calculated from the interaction solutions are greater than those calculated for the completely rigid airplane, whereas, for airplane B, the converse is true. This result for airplane B is due to two factors: (a) the dynamic amplification factor is less than unity because of the relatively large natural period of the airplane compared with the duration of the impact pulse ($t_i/t_n \approx 0.3$), and (b) there is considerable reduction in the magnitude of the landing-gear force because of the effects of interaction. In the case of airplane B, the natural period is of about the same duration as the impact pulse ($t_i/t_n \approx 1.1$) so that the dynamic magnification factor is considerably greater than unity and more than overcomes the effect of the reduction in landing-gear force.

From the preceding results, it can be seen that the effects of structural flexibility are twofold; namely, (a) a change in the magnitude of the applied landing-gear force due to interaction, the amount depending on the natural frequency of the structure, the mass ratio m_s/m_f, and the landing-gear characteristics, and (b) either dynamic amplification or attenuation of the loads in the structure compared with those for a rigid body, depending largely on the ratio of the duration of the impact pulse to the natural period of the structure. In the particular examples considered, the landing-gear force was reduced by the effects of interaction;

it is conceivable, however, that, for some combinations of landing-gear and airplane characteristics, perhaps when the natural period of the structure is smaller than the duration of the impact pulse and the mass ratio is large, interaction may result in an increase in the maximum landing-gear force over that for a rigid airplane because of the superposition of oscillations of the landing-gear attachment point on the motions of the shock strut. Such an unfavorable effect of structural flexibility on the applied force was indicated for certain cases of seaplane impact in reference 7.

In view of the foregoing observations it would appear worthwhile to consider the effects of interaction in dynamic analyses of landing loads when the landing gear is located at points in the airplane that experience appreciable deflections relative to the mass center of the system.

CONCLUSIONS

The effects of interaction between a landing gear and a flexible airplane structure on the behavior of the landing gear and the loads in the structure have been studied by treating the equations of motion of the airplane and the landing gear as a coupled system. The landing gear is considered to have nonlinear characteristics typical of conventional gears, namely, velocity-squared damping, polytropic air-compression springing, and exponential tire force-deflection characteristics. For the case where only two modes of the structure are considered, an equivalent three-mass system is derived for representing the airplane and landing-gear combination, which may be used to simulate the effects of structural flexibility in jig drop tests of landing gears.

As examples to illustrate the effects of interaction, numerical calculations, based on the structural properties of two large airplanes having considerably different mass and flexibility characteristics, are presented. In order to cover a range of parameters, the landing gear of each airplane was assumed to be located at three arbitrary spanwise positions in addition to its original location. For the particular cases considered, it was found that

1. The effects of interaction can result in appreciable reductions in the magnitude of the landing-gear force, particularly when the flexibility of the airplane structure is large and the natural frequency of the structure is small.

2. Neglect of interaction effects, that is, the use of the landing-gear forcing function for a rigid airplane in a dynamic analysis of a flexible airplane, can lead to the calculation of excessive loads in the airplane structure.

3. In the case of one of the airplanes, the structural loads calculated from the interaction solutions are greater than those for a completely rigid airplane treatment (rigid structure subjected to rigid-body forcing function) because of the fact that the effects of dynamic magnification more than overcome the reduction in landing-gear force due to interaction. In the case of the second airplane, because of the relatively large natural period of the structure in comparison with the duration of the impact pulse, the dynamic magnification factor is appreciably less than unity. This effect, coupled with the reductions in landing-gear force due to interaction, results in structural loads that are less than those for a rigid airplane.

It thus appears desirable to consider the effects of interaction in dynamic analyses of landing loads for large airplanes, particularly when the landing-gear attachment points experience large deflections relative to the mass center of the airplane.

Langley Aeronautical Laboratory,
National Advisory Committee for Aeronautics,
Langley Field, Va., May 5, 1955.

APPENDIX A

CONDITIONS AT BEGINNING OF SHOCK-STRUT MOTION

Since the shock strut does not begin to deflect until the preloading force imposed by the internal air pressure is overcome by the inertia forces, the shock strut is essentially rigid during the interval between the instant of initial contact with the ground and the beginning of shock-strut motion at some time $t = t_\tau$. During this interval, since the deflection of the tire is essentially the same as the displacement of the landing-gear attachment point, the system used in the numerical calculations to represent the airplane and landing-gear combination has only two degrees of freedom, namely, the rigid-body or zero-mode displacement and the deflection in the first flexible mode, the higher modes being neglected. The purpose of this appendix is to consider the motions of the system prior to the beginning of shock-strut deflection in order to determine the conditions which exist at the instant the shock strut first begins to move; these motions then serve as the initial conditions for the equations of motion of the system during the main part of the impact. For this purpose it may be reasonably assumed that the tire force-deflection relationship is linear for the relatively small range of deflection prior to the beginning of shock-strut motion and that, therefore, $F_{V_g}(z_f) = m'z_f$. In order to avoid a step jump in the time-history solution at the time t_τ, the constant m' should be determined so that

$$m'z_{f_\tau} = mz_{f_\tau}{}^r \tag{A1}$$

Distributed System

Prior to time t_τ the equations of motion for the airplane and landing gear are given by equations (18) with initial conditions:

$$z_f(0) = a_0(0) = a_1(0) = 0$$

$$\dot{z}_f(0) = \dot{a}_0(0) = V_{V_o}$$

$$\dot{a}_1(0) = 0$$

Since $a_1 = \frac{z_f - a_0}{\xi_1}$, equations (18) can be written as

$$M_0\ddot{a}_0 = -m'z_f - m_u\ddot{z}_f + W_u - Z_0 \tag{A2a}$$

$$\frac{M_1}{\xi_1^2}\ddot{a}_0 + \frac{M_1\omega_1^2}{\xi_1^2}a_0 = \left(\frac{M_1}{\xi_1^2} + m_u\right)\ddot{z}_f + \left(\frac{M_1\omega_1^2}{\xi_1^2} + m'\right)z_f \tag{A2b}$$

The exact solution of equations (A2) can be shown to be

$$z_f(t) = \frac{1}{A^2 - B^2}\left\{V_{V_0}\left(\frac{A^2 - C}{A}\sin At - \frac{B^2 - C}{B}\sin Bt\right) + D\left[\frac{\omega_1^2 - A^2}{A^2}\cos At - \frac{\omega_1^2 - B^2}{B^2}\cos Bt + \omega_1^2\left(\frac{1}{B^2} - \frac{1}{A^2}\right)\right]\right\} \tag{A3}$$

where

$$A = \sqrt{\frac{E - \sqrt{E^2 - 4F}}{2}}$$

$$B = \sqrt{\frac{E + \sqrt{E^2 - 4F}}{2}}$$

$$C = \frac{M_1\omega_1^2(M_0 + m_u)}{G}$$

$$D = \frac{M_1(W_u - Z_0)}{G}$$

$$E = \frac{m'\left(M_1 + M_0\xi_1^2\right)}{G} + C$$

$$F = \frac{m'M_1\omega_1^2}{G}$$

$$G = M_1(M_0 + m_u) + m_uM_0\xi_1^2$$

By successive differentiation of equation (A3), the higher derivatives of $z_f(t)$ are found to be

$$\dot{z}_f(t) = \frac{1}{A^2 - B^2}\left\{V_{V_o}\left[(A^2 - C)\cos At - (B^2 - C)\cos Bt\right] + D\left[\left(\frac{\omega_1^2 - B^2}{B}\right)\sin Bt - \left(\frac{\omega_1^2 - A^2}{A}\right)\sin At\right]\right\} \tag{A4}$$

$$\ddot{z}_f(t) = \frac{1}{A^2 - B^2}\left\{V_{V_o}\left[B(B^2 - C)\sin Bt - A(A^2 - C)\sin At\right] + D\left[\left(\omega_1^2 - B^2\right)\cos Bt - (\omega^2 - A^2)\cos At\right]\right\} \tag{A5}$$

$$\dddot{z}_f(t) = \frac{1}{A^2 - B^2}\left\{V_{V_o}\left[B^2(B^2 - C)\cos Bt - A^2(A^2 - C)\cos At\right] + D\left[A\left(\omega_1^2 - A^2\right)\sin At - B\left(\omega_1^2 - B^2\right)\sin Bt\right]\right\} \tag{A6}$$

At the time t_T, the equation of motion of the unsprung mass of the landing gear as a free body is given by equation (2) which, with $F_{V_g} = m'z_f$, may be written as

$$m_u\ddot{z}_{f_T} + m'z_{f_T} = p_{a_o}A_a \cos\theta + W_u \tag{A7}$$

Substituting for z_{f_T} and $\ddot{z}_{f_T}$ in equation (A7) gives a relationship between t_T and m':

$$\frac{1}{A^2 - B^2}\left\{V_{V_o}\left[\frac{A^2 - C}{A}(m' - m_uA^2)\sin At - \frac{B^2 - C}{B}(m' - m_uB^2)\sin Bt\right] + \right.$$

$$D\left[\frac{\omega_1^2 - A^2}{A^2}(m' - m_uA^2)\cos At - \frac{\omega_1^2 - B^2}{B^2}(m' - m_uB^2)\cos Bt + \right.$$

$$\left.\left. m'\omega_1^2\left(\frac{1}{B^2} - \frac{1}{A^2}\right)\right]\right\} = p_{a_o}A_a \cos\theta + W_u \tag{A8}$$

Because equation (A8) is transcendental in both t_T and m' (m' being involved in the constants A and B), in order to obtain an explicit solution for t_T or m', some approximation to the trigonometric terms is necessary, the order of the approximation depending on the accuracy required. For the determination of t_T and m' it will generally be sufficient to assume first-order approximations for the trigonometric terms where only the first terms of their series expansions are used. With these approximations the solution of equation (A8) for t_T is

$$t_T = \frac{G\left(p_{a_o}A_a \cos\theta + W_u - Dm_u\right)}{m'M_1M_oV_{V_o}} \tag{A9}$$

As indicated previously, m' cannot be chosen arbitrarily but must be determined in accordance with equation (A1), which may be written as

$$m' = mz_{f_T}^{r-1}$$

The first-order approximation for z_{f_τ}, obtained from equation (A3), is

$$z_{f_\tau} = V_{V_o} t_\tau \tag{A10}$$

With these substitutions equation (A9) may be written as

$$t_\tau = \frac{1}{V_{V_o}} \left[\frac{G\left(p_{a_o} A_a \cos \theta + W_u - D m_u\right)}{m M_1 M_o} \right]^{1/r} \tag{A11}$$

and the equation for m' becomes

$$m' = m^{1/r} \left[\frac{G\left(p_{a_o} A_a \cos \theta + W_u - D m_u\right)}{M_1 M_o} \right]^{\frac{r-1}{r}} \tag{A12}$$

The first-order approximations for the derivatives of z_f at time t_τ, from equations (A4) to (A6), are

$$\dot{z}_{f_\tau} = V_{V_o} + D t_\tau \tag{A13}$$

$$\ddot{z}_{f_\tau} = V_{V_o} \left[C - \left(A^2 + B^2\right) \right] t_\tau + D \tag{A14}$$

and

$$\dddot{z}_{f_\tau} = V_{V_o} \left[C - \left(A^2 + B^2\right) \right] + t_\tau D \left[\omega_1^2 - \left(A^2 + B^2\right) \right] \tag{A15}$$

With the values of t_τ and m' calculated from equations (A11) and (A12), the values of $z_{f_\tau} = z_{u_\tau}$, $\dot{z}_{f_\tau} = \dot{z}_{u_\tau}$, and $\ddot{z}_{f_\tau} = \ddot{z}_{u_\tau}$ can be calculated from equations (A10), (A13), and (A14), respectively. These values provide two-thirds of the initial conditions for the process subsequent to the beginning of shock-strut deflection (eq. 19). The

remaining initial conditions, for example, a_{0_τ}, $\dot{a}_{0_\tau}$, and $\ddot{a}_{0_\tau}$, can be obtained by manipulation of the differential equations (A2). From equation (A2b) it can be seen that

$$a_{0_\tau} = \frac{\xi_1^2}{M_1\omega_1^2}\left[\left(\frac{M_1}{\xi_1^2} + m_u\right)\ddot{z}_{f_\tau} + \left(\frac{M_1\omega_1^2}{\xi_1^2} + m'\right) z_{f_\tau} - \frac{M_1}{\xi_1^2}\,\ddot{a}_{0_\tau}\right] \tag{A16}$$

By differentiation,

$$\dot{a}_{0_\tau} = \frac{\xi_1^2}{M_1\omega_1^2}\left[\left(\frac{M_1}{\xi_1^2} + m_u\right)\dddot{z}_{f_\tau} + \left(\frac{M_1\omega_1^2}{\xi_1^2} + m'\right) \dot{z}_{f_\tau} - \frac{M_1}{\xi_1^2}\,\dddot{a}_{0_\tau}\right] \tag{A17}$$

where, from equation (A2a),

$$\left.\begin{aligned} \ddot{a}_{0_\tau} &= -\frac{m' z_{f_\tau} + m_u \ddot{z}_{f_\tau} - W_u + Z_0}{M_0} \\ &= -\frac{p_{a_o} \cos\theta + Z_0}{M_0} \end{aligned}\right\} \tag{A18}$$

Differentiating equation (A2a) gives

$$\dddot{a}_{0_\tau} = -\frac{m' z_{f_\tau} + m_u \dddot{z}_{f_\tau}}{M_0} \tag{A19}$$

The substitution of equations (A18) and (A19) and the initial conditions previously determined $\left(z_{f_\tau},\ \dot{z}_{f_\tau},\ \ddot{z}_{f_\tau},\ \text{and}\ \dddot{z}_{f_\tau}\right)$ into equations (A16) to (A18) provides the remaining initial conditions for the second phase of the impact.

Equivalent Three-Mass System

The equations of motion for the equivalent three-mass system prior to the time t_T are equations (20) with initial conditions

$$z_f(0) = z_s(0) = 0$$

and

$$\dot{z}_f(0) = \dot{z}_s(0) = V_{V_O}$$

Since it has been shown that equations (20) are identically equivalent to equations (18) for the distributed system when the relationships between the constants of the two systems are as defined by equations (27) to (34), it follows that equations (A3) to (A15) are equally valid for the three-mass system when the constants are redefined in accordance with equations (27) to (34). The redefined constants, in terms of the properties of the three-mass system, may be written as

$$C = \frac{m_f \omega_1^2 (M_O + m_u)}{M_O (m_f + m_u)}$$

$$D = \frac{m_f (W_u - Z_O)}{M_O (m_f + m_u)}$$

$$E = \frac{m'}{m_f + m_u} + C$$

$$F = \frac{m_f m' \omega_1^2}{M_O (m_f + m_u)}$$

where

$$M_O = m_f + m_s$$

and

$$\omega_1 = \sqrt{\frac{kM_o}{m_f m_s}}$$

The equations for t_τ and m', equations (A11) and (A12), become

$$t_\tau = \frac{1}{V V_o}\left[\frac{H\left(p_{a_o} A_a \cos\theta + W_u - Dm_u\right)}{m}\right]^{1/r} \tag{A20}$$

where

$$H = \frac{m_f + m_u}{m_f}$$

and

$$m' = m^{1/r}\left[H\left(p_{a_o} A_a \cos\theta + W_u - Dm_u\right)\right]^{\frac{r-1}{r}} \tag{A21}$$

The values of t_τ and m' given by these equations permit the calculation of $z_{f_\tau} = z_{u_\tau}$, $\dot{z}_{f_\tau} = \dot{z}_{u_\tau}$, and $\ddot{z}_{f_\tau} = \ddot{z}_{u_\tau}$ by means of equations (A10), (A13), and (A14). The remaining initial conditions for the second phase of the impact, z_s and its derivatives at the time t_τ, can be obtained by manipulation of the differential equations (20). Solving equation (20a) for z_s at time t_τ gives

$$z_{s_\tau} = \frac{1}{k}\left[(m_f + m_u)\ddot{z}_{f_\tau} + (k + m')z_{f_\tau} + L_f + W_f - W_u\right] \tag{A22}$$

Differentiating equation (20a) and substituting $FV_g(z_f) = m'z_f$ gives

$$\dot{z}_{s_\tau} = \frac{1}{k}\left[(m_f + m_u)\dddot{z}_{f_\tau} + (k - m')\dot{z}_{f_\tau}\right] \tag{A23}$$

An expression for $\ddot{z}_{s_\tau}$ can easily be obtained from equation (20b) as follows:

$$\ddot{z}_{s_\tau} = -\frac{1}{m_s}\left[(m_f + m_u)\ddot{z}_{f_\tau} + m'z_{f_\tau} + (L_s + L_f) - (W_s + W_f + W_u)\right] \quad (A24)$$

Equations (A22) to (A24), in conjunction with the values of z_{f_τ}, $\dot{z}_{f_\tau}$, and $\ddot{z}_{f_\tau}$ previously determined, supply all the initial conditions for the second phase of the impact of the equivalent three-mass system.

APPENDIX B

DYNAMIC LOADS IN AIRPLANE STRUCTURE

The equations of motion of the airplane have been previously presented in several forms so that solutions for the motions of the structure can be obtained in terms of the variables a_0 and a_1, a_0 and z_f, or z_f and z_s. The purpose of this section is to present equations from which the accelerations, bending moments, and shears at any point on the airplane structure can be calculated once the time-history solutions for the basic variables have been obtained.

Acceleration

At any point.- The absolute displacement at any point on the structure (see fig. 2) is

$$z = w + x\varphi$$

Since

$$w = a_0 + a_1 w_1$$

and

$$\varphi = a_1 \varphi_1$$

where w_1 and φ_1 are the modal functions for bending and torsion, respectively,

$$z = a_0 + a_1(w_1 + x\varphi_1)$$

and

$$\ddot{z} = \ddot{a}_0 + \ddot{a}_1(w_1 + x\varphi_1) \qquad \text{(B1)}$$

Since

$$\ddot{a}_1 = \frac{\ddot{z}_f - \ddot{a}_0}{\xi_1}$$

the acceleration at any point may also be written as

$$\ddot{z} = \ddot{a}_0 + (\ddot{z}_f - \ddot{a}_0)\frac{w_1 + x\varphi_1}{\xi_1} \tag{B2}$$

Since, from equation (36)

$$\ddot{a}_0 = \frac{m_f\ddot{z}_f + m_s\ddot{z}_s}{M_0}$$

the acceleration can also be written as

$$\ddot{z} = \frac{1}{M_0}\left[m_f\ddot{z}_f + m_s\ddot{z}_s + m_s(\ddot{z}_f - \ddot{z}_s)\frac{w_1 + x\varphi_1}{\xi_1}\right] \tag{B3}$$

Along elastic axis.- At the elastic axis, the displacement is designated w and $x = 0$ so that equation (B1) becomes simply

$$\ddot{w} = \ddot{a}_0 + \ddot{a}_1 w_1 \tag{B4}$$

Equation (B2) becomes

$$\ddot{w} = \ddot{a}_0 + (\ddot{z}_f - \ddot{a}_0)\frac{w_1}{\xi_1} \tag{B5}$$

Equation (B3) becomes

$$\ddot{w} = \frac{1}{M_0}\left[m_f\ddot{z}_f + m_s\ddot{z}_s + m_s(\ddot{z}_f - \ddot{z}_s)\frac{w_1}{\xi_1}\right] \tag{B6}$$

Along station mass centers.- At the mass center of any station the displacement is designated ζ and $x = \epsilon$ so that equation (B1) becomes

$$\ddot{\zeta} = \ddot{a}_0 + \ddot{a}_1\zeta_1 \tag{B7}$$

where ζ_1 is the modal function for the station mass centers and is equal to $w_1 + e\varphi_1$. Equation (B2) becomes

$$\ddot{\zeta} = \ddot{a}_0 + (\ddot{z}_f - \ddot{a}_0)\frac{\zeta_1}{\xi_1} \tag{B8}$$

Equation (B3) becomes

$$\ddot{\zeta} = \frac{1}{M_0}\left[m_f\ddot{z}_f + m_s\ddot{z}_s + m_s(\ddot{z}_f - \ddot{z}_s)\frac{\zeta_1}{\xi_1}\right] \tag{B9}$$

Bending Moments

Outboard of landing gear.- The bending moment at any spanwise station y_j outboard of the landing-gear station y_g is readily determined by summing up the inertia moments produced by the accelerations of the mass centers of all stations i between station y_j and the tip. Thus,

$$(BM)_{y_j \geq y_g} = \sum_{i=j}^{tip} m_i\ddot{\zeta}_i(y_i - y_j) \tag{B10}$$

Inboard of landing gear.- The bending moment at any spanwise station y_j inboard of the landing-gear station y_g is equal to the sum of the inertia moments produced by the accelerations of the mass centers of all stations i between station y_j and the tip plus the moment produced by the landing-gear force. Thus,

$$(BM)_{y_j \leq y_g} = \sum_{i=j}^{tip} m_i \ddot{\zeta}_i (y_i - y_j) + F(y_g - y_j) \tag{B11}$$

Inasmuch as

$$F = -(M_0 \ddot{a}_0 + Z_0)$$

equation (B11) can also be written as

$$(BM)_{y_j \leq y_g} = \sum_{i=j}^{tip} m_i \ddot{\zeta}_i (y_i - y_j) - (M_0 \ddot{a}_0 + Z_0)(y_g - y_j) \tag{B12}$$

Shears

Outboard of landing gear.- The vertical shear at any spanwise station y_j outboard of the landing-gear station y_g is simply the sum of the inertia reactions due to the accelerations of the mass centers of all stations i between station y_j and the tip. Thus,

$$S_{y_j \geq y_g} = \sum_{i=j}^{tip} m_i \ddot{\zeta}_i \tag{B13}$$

Inboard of landing gear.- The vertical shear at any spanwise station y_j inboard of the landing-gear station y_g is the sum of the inertia reactions due to the accelerations of the mass centers of all stations i between station y_j and the tip plus the landing-gear force. Thus,

$$S_{y_j \leq y_g} = \sum_{i=j}^{tip} m_i \ddot{\zeta}_i + F$$

$$= \sum_{i=j}^{tip} m_i \ddot{\zeta}_i - (M_0 \ddot{a}_0 + Z_0) \tag{B14}$$

APPENDIX C

RESPONSE TO GIVEN FORCING FUNCTIONS

In this appendix equations are presented for the acceleration response of the airplane structure to predetermined forcing functions applied by the landing gear. The cases considered are the arbitrary forcing function, the sine pulse, and a pulse made up of sine and cosine segments. For the particular case where the landing-gear forcing function can be represented by a single sine pulse,

$$F(t) = F_{max} \sin \Omega t$$

where Ω is the circular frequency of the applied sine pulse and is expressed by

$$\Omega = \frac{\pi}{2T}$$

where T is the time to reach F_{max}.

If the forcing pulse is not symmetrical in time about its maximum value, it may be represented by a combined pulse consisting of a sine function up to the time T and a cosine function subsequent to the time T. This latter function may be written as

$$F(t') = F_{max} \cos \Omega_1 t' \qquad t' \geq 0$$

where

$$t' = t - T$$

and Ω_1 is the circular frequency of the cosine pulse; the initial conditions are the same as the conditions at the time $t = T$ determined from the response to the sine-function segment of the pulse.

The solutions are presented for the distributed system of the airplane (sketch a) and for the equivalent concentrated-mass system (sketch b)

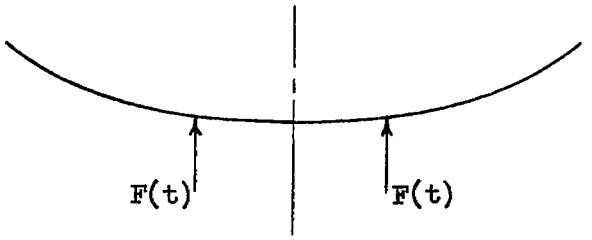

(a) Distributed system.

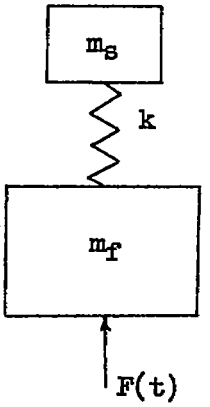

(b) Concentrated-mass system.

Distributed System

The acceleration response of the rigid body or zero mode is immediately evident from the equation of motion for $n = 0$, namely,

$$\ddot{a}_0 = - \frac{F(t) + Z_0}{M_0}$$

The response of the deflection modes follows.

Arbitrary forcing function.- When the landing-gear forcing function is predetermined and arbitrary, the equation of motion for the nth mode (eq. (15a)) can be written as

$$M_n \ddot{a}_n + M_n \omega_n^2 a_n = - \left[F(t) + W_u \right] \xi_n \qquad (n \neq 0) \qquad (C1)$$

where $F(t)$ is an arbitrary function of time and a_n is the generalized coordinate of the nth mode.

The general solution of equation (C1) may be written as

$$a_n(t) = -\frac{\xi_n}{M_n\omega_n}\int_0^t F(\tau)\sin\omega_n(t-\tau)d\tau + \frac{W_u\xi_n}{M_n\omega_n^2}(\cos\omega_n t - 1) +$$

$$a_n(0)\cos\omega_n t + \frac{\dot{a}_n(0)}{\omega_n}\sin\omega_n t \qquad (C2)$$

The acceleration response is obtained by double differentiating equation (C2) as follows:

$$\ddot{a}_n(t) = \frac{\xi_n}{M_n}\left[F(t) - \omega_n\int_0^t F(\tau)\sin\omega_n(t-\tau)d\tau + W_u\cos\omega_n t\right] -$$

$$a_n(0)\omega_n^2\cos\omega_n t - \ddot{a}_n(0)\omega_n\sin\omega_n t \qquad (C3)$$

Equations (C2) and (C3) are general solutions to equation (C1) and thus represent the response of any mode to an arbitrary forcing function $F(t)$. In the present study of landing impact, the initial conditions are

$$a_n(0) = 0$$

and

$$\dot{a}_n(0) = 0$$

Sine-pulse forcing function.- For the particular case where the forcing function is a sine pulse, the acceleration response, as determined from equation (C3), is

$$\ddot{a}_n(t) = F_{max}\frac{\xi_n}{M_n}\left[\frac{\omega_n}{\Omega^2 - \omega_n^2}(\Omega\sin\omega_n t - \omega_n\sin\Omega t) - \sin\Omega t\right] -$$

$$\left(\frac{W_u\xi_n}{M_n} + a_n(0)\omega_n^2\right)\cos\omega_n t - \dot{a}_n(0)\omega_n\sin\omega_n t \qquad (C4)$$

where, again, $a_n(0) = 0$ and $\dot{a}_n(0) = 0$.

Half-sine—half-cosine pulse.- In this case the response up to time T is given by equation (C4). Subsequent to time T the acceleration response, determined from equation (C3), may be written as

$$a_n(t') = F_{max}\frac{\xi_n}{M_n}\left[\frac{\omega_n^2}{\Omega_1^2 - \omega_n^2}(\cos \omega_n t' - \cos \Omega_1 t') - \cos \Omega_1 t'\right] -$$

$$\left[\frac{W_u \xi_n}{M_n} + a_n(0)\omega_n^2\right]\cos \omega_n t' - \dot{a}_n(0)\omega_n \sin \omega_n t' \qquad (C5)$$

where

$$t' = (t - T) \geq 1$$

$$a_n(0) = a_{n_T}$$

$$\dot{a}_n(0) = \dot{a}_{n_T}$$

Equivalent Concentrated-Mass System

The equations of motion for the concentrated-mass system subject to an arbitrary forcing function are (see eqs. (22))

$$\left.\begin{aligned} m_f\ddot{z}_f - k(z_s - z_f) + L_f - W_f &= - F(t) \\ m_f\ddot{z}_f + m_s\ddot{z}_s + (L_f + L_s) - (W_s + W_f) &= - F(t) \end{aligned}\right\} \qquad (C6)$$

Introducing the new variable

$$u = z_s - z_f$$

permits the combination of equations (C6) into a single equation in one variable:

$$m_f\ddot{u} + k\left(1 + \frac{m_f}{m_s}\right)u = F(t) + J \tag{C7}$$

where

$$J = L_f - W_f - \frac{m_f}{m_s}(L_s - W_s)$$

The solution of equation (C7), by analogy with equation (C1), can be written as

$$u(t) = \frac{1}{m_f\omega_1}\int_0^t F(\tau)\sin\omega_1(t - \tau)d\tau + \frac{J}{m_f\omega_1^2}(1 - \cos\omega_1 t) +$$

$$u(0)\cos\omega_1 t + \frac{\dot{u}(0)}{\omega_1}\sin\omega_1 t \tag{C8}$$

where

$$\omega_1^2 = k\frac{M_0}{m_f m_s}$$

By substituting $u(t)$ for $z_s - z_f$ in equations (C6) and combining, the following equations for the responses $\ddot{z}_s$ and $\ddot{z}_f$ can be obtained:

$$\ddot{z}_s(t) = -\frac{k}{m_s}\left[\frac{1}{m_f\omega_1}\int_0^t F(\tau)\sin\omega_1(t - \tau)d\tau + \frac{J}{m_f\omega_1^2}(1 - \cos\omega_1 t) +\right.$$

$$\left. u(0)\cos\omega_1 t + \frac{\dot{u}(0)}{\omega_1}\sin\omega_1 t\right] + \frac{W_s - L_s}{m_s} \tag{C9}$$

and

$$\ddot{z}_f(t) = \frac{1}{m_f}\left\{-\left[F(t) + (L_f - W_f)\right] + k\left[\frac{1}{m_f\omega_1}\int_0^t F(\tau)\sin\omega_1(t-\tau)d\tau + \right.\right.$$

$$\left.\left.\frac{J}{m_f\omega_1^2}(1 - \cos\omega_1 t) + u(0)\cos\omega_1 t + \frac{\dot{u}(0)}{\omega_1}\sin\omega_1 t\right]\right\} \qquad (C10)$$

In equations (C9) and (C10), $u(0) = \dot{u}(0) = 0$ for the present application to landing impact.

Sine-pulse forcing function.- For the case where the forcing term is a sine pulse, equations (C9) and (C10) become

$$\ddot{z}_s(t) = -\frac{k}{m_s}\left[\frac{F_{max}(\Omega\sin\omega_1 t - \omega_1\sin\Omega t)}{m_f\omega_1(\Omega^2 - \omega_1^2)} + \frac{J}{m_f\omega_1^2}(1 - \cos\omega_1 t) + \right.$$

$$\left. u(0)\cos\omega_1 t + \frac{\dot{u}(0)}{\omega_1}\sin\omega_1 t\right] + \frac{W_s - L_s}{m_s} \qquad (C11)$$

and

$$\ddot{z}_f(t) = \frac{1}{m_f}\left\{F_{max}\left[\frac{k(\Omega\sin\omega_1 t - \omega_1\sin\Omega t)}{m_f\omega_1(\Omega^2 - \omega_1^2)} - \sin\Omega t\right] - (L_f - W_f) + \right.$$

$$\left.\frac{Jk(1 - \cos\omega_1 t)}{m_f\omega_1^2} + k\left[u(0)\cos\omega_1 t + \frac{\dot{u}(0)}{\omega_1}\sin\omega_1 t\right]\right\} \qquad (C12)$$

where, again, $u(0) = \dot{u}(0) = 0$.

Half-sine—half-cosine pulse.- The response up to time T is given by equations (C11) and (C12). Subsequent to time T, the responses (eqs. (C9) and (C10)) become

$$\ddot{z}_s(t') = -\frac{k}{m_s}\left[\frac{F_{max}(\cos \omega_1 t' - \cos \Omega t')}{m_f\left(\Omega_1^2 - \omega_1^2\right)} + \frac{J}{m_f\omega_1^2}(1 - \cos \omega_1 t') + u(0)\cos \omega_1 t' + \frac{\dot{u}(0)}{\omega_1} \sin \omega_1 t'\right] + \frac{W_s - L_s}{m_s} \tag{C13}$$

and

$$\ddot{z}_f(t') = \frac{1}{m_f}\left\{F_{max}\left[\frac{k(\cos \omega_1 t' - \cos \Omega_1 t')}{m_f\left(\Omega_1^2 - \omega_1^2\right)} - \cos \Omega_1 t'\right] - (L_f - W_f) + \frac{Jk(1 - \cos \omega_1 t')}{m_f\omega_1^2} + k\left[u(0)\cos \omega_1 t + \frac{\dot{u}(0)}{\omega_1} \sin \omega_1 t'\right]\right\} \tag{C14}$$

where

$$t' = t - T = 0$$

$$u(0) = u_T$$

$$\dot{u}(0) = \dot{u}_T$$

APPENDIX D

AERODYNAMIC AND WEIGHT MOMENTS AND SHEARS

In appendix B equations were presented for the bending moments and shears due to the combination of the inertia forces arising from the accelerations of the masses distributed along the span and the landing-gear force. In the calculation of the total moments and shears, however, consideration must be given to the aerodynamic lift and weight forces. This appendix presents equations for estimating these aerodynamic and weight moments and shears which, although only first approximations, are considered sufficiently accurate for the purposes of the present study.

If it is assumed that the lift coefficient is constant along the span and equal to the average lift coefficient of the wing C_L, the lift force at any station y_i is equal to $C_L \frac{\rho}{2} V_L^2 A_i$ where A_i is the area assumed to be concentrated at the station.

The moment at any station y_j due to the lift and weight forces at each station i outboard of station y_j is

$$(M_a)_{y_j} = C_L \frac{\rho}{2} V_L^2 \sum_{i=j}^{tip} A_i(y_i - y_j) - g \sum_{i=j}^{tip} m_i(y_i - y_j) \qquad (D1)$$

If unsteady-state lift effects are neglected, the instantaneous lift coefficient is related to the lift coefficient at the instant of initial contact by the expression

$$C_L = C_{L_o} + C_{L_\alpha}(\gamma - \gamma_o)$$

$$= C_{L_o} + C_{L_\alpha}\left(\frac{\dot{a}_o - VV_o}{V_L}\right)$$

Inasmuch as the total lift at the instant of contact is

$$\int_0^{b/2} L\, dy = Z_o + M_o g,$$

$$C_{L_o} = \frac{Z_o + M_o g}{\frac{\rho}{2} A V_L^2}$$

so that

$$(M_a)_{y_j} = \left[\frac{Z_0 + M_0 g}{A} + C_{L_\alpha}\left(\dot{a}_0 - V_{V_0}\right)\frac{\rho}{2} V_L\right] \sum_{i=j}^{tip} A_i(y_i - y_j) -$$

$$g \sum_{i=j}^{tip} m_i(y_i - y_j) \tag{D2}$$

Similarly, the shear at any station y_j is

$$(S_a)_{y_j} = \left[\frac{Z_0 + M_0 g}{A} + C_{L_\alpha}\left(\dot{a}_0 - V_{V_0}\right)\frac{\rho}{2} V_L\right] \sum_{i=j}^{tip} A_i - g \sum_{i=j}^{tip} m_i \tag{D3}$$

REFERENCES

1. Fairthorne, R. A.: The Effects of Landing Shock on Wing and Undercarriage Deflexion. R. & M. No. 1877, British A.R.C., 1939.

2. Stowell, Elbridge Z., Houbolt, John C., and Batdorf, S. B.: An Evaluation of Some Approximate Methods of Computing Landing Stresses in Aircraft. NACA TN 1584, 1948.

3. McPherson, Albert E., Evans, J., Jr., and Levy, Samuel: Influence of Wing Flexibility on Force-Time Relation in Shock Strut Following Vertical Landing Impact. NACA TN 1995, 1949.

4. Pian, T. H. H., and Flomenhoft, H. I.: Analytical and Experimental Studies on Dynamic Loads in Airplane Structures During Landing. Jour. Aero. Sci., vol. 17, no. 12, Dec. 1950, pp. 765-774, 786.

5. O'Brien, T. F., and Pian, T. H. H.: Effect of Structural Flexibility on Aircraft Loading. Part 1. Ground-Loads. AF Tech. Rep. No. 6358, pt. 1, WADC, U. S. Air Force, M.I.T., July 1951.

6. Milwitzky, Benjamin, and Cook, Francis E.: Analysis of Landing-Gear Behavior. NACA Rep. 1154, 1953. (Supersedes NACA TN 2755.)

7. Mayo, Wilbur L.: Hydrodynamic Impact of a System With a Single Elastic Mode. I - Theory and Generalized Solution With an Application to an Elastic Airframe. NACA Rep. 1074, 1952. (Supersedes NACA TN 1398.)

8. Biot, M. A., and Bisplinghoff, R. L.: Dynamic Loads on Airplane Structures During Landing. NACA WR W-92, 1944. (Formerly NACA ARR 4H10.)

9. Lawrence, H. R.: The Dynamics of a Swept Wing. Jour. Aero. Sci., vol. 14, no. 11, Nov. 1947, pp. 643-650.

10. Isakson, G.: A Survey of Analytical Methods for Determining Transient Stresses in Elastic Structures. Contract No. N5 ori-07833, Office Naval Res. (Project NR-035-259), M.I.T., Mar. 3, 1950.

11. Southwell, R. V.: Relaxation Methods in Theoretical Physics. The Clarendon Press (Oxford), 1946.

12. Scarborough, James B.: Numerical Mathematical Analysis. Second ed., The Johns Hopkins Press (Baltimore), 1950.

13. Levy, H., and Baggott, E. A.: Numerical Solutions of Differential Equations. First Am. ed., Dover Pub. Inc., 1950.

TABLE I.- CHARACTERISTICS OF AIRPLANE A

(a) Structure

[Data taken from ref. 8]

Station, in.	m_i, $\frac{lb\text{-}sec^2}{in.}$	I_{ea_i}, lb-in.-sec^2	ϵ_i, in.	W_{l_i}	φ_{l_i}
0	28.5	-------	0	-0.078	0
133	16.3	85,234	-39.26	-.031	-.00084
217	5.27	1,288	0	-.047	-.0016
307	9.15	61,717	-62.19	.164	-.00183
428	.974	536	0	.374	-.00185
548	.686	287	0	.670	-.00187
638	.153	34.1	0	.936	-.00188

M_0, $\frac{lb\text{-}sec^2}{in.}$ 61.033

M_1, $\frac{lb\text{-}sec^2}{in.}$ 1.607

f_1, cps 3.365

(b) Shock strut

[Manufacturer's data]

A_h, sq ft 0.163

A_a, sq ft 0.214

A_n, sq ft 0.00173

v_o, cu ft 0.2597

p_{a_o}, lb/sq ft 30,528

ρ, slugs/cu ft 1.626

(c) Unsprung mass

[Manufacturer's data]

W_u, lb 700

Tires (one per landing gear) . . . . . 56-inch smooth contour

Tire pressure, lb/sq in. 70

m, lb/ft 85,309

r 1.22

TABLE II.- CHARACTERISTICS OF AIRPLANE B

(a) Structure

[Unpublished data]

Station, in.	m_i, $\frac{\text{lb-sec}^2}{\text{in.}}$	I_{ea_i}, lb-in.-sec^2	e_i, in.	W_{l_i}	φ_{l_i}
0	109.534	4,475,280	200.37	-0.0585	-0.000176
84	4.695	3,046	-4.65	-.0579	-.000187
168	4.920	19,490	-24.20	-.0350	-.000204
252	22.177	278,942	-101.22	.0037	-.000231
336	2.560	2,161	2.44	.090	-.000272
420	2.557	1,988	2.60	.1842	-.000322
504	1.773	1,136	.92	.3253	-.000379
588	3.269	2,474	-14.79	.4772	-.000435
672	8.628	8,439	-26.88	.6369	-.000482
756	1.144	500	.60	.8181	-.000514
840	.520	186	5.48	1.000	-.000526

M_O, $\frac{\text{lb-sec}^2}{\text{in.}}$ 161.775

M_1, $\frac{\text{lb-sec}^2}{\text{in.}}$ 6.9096

f_1, cps 1.29

(b) Shock strut

[Values estimated from generalized curves of ref. 6]

$\frac{\rho A_h^3}{2(C_d A_n)^2}$, $\frac{\text{slugs}}{\text{ft}}$ 17,900

A_a, sq ft 0.585

v_o, cu ft 0.7095

p_{a_o}, lb/sq ft 30,528

(c) Unsprung Mass

[Manufacturer's data]

W_u, lb 2,300

Tires (two per landing gear) . . . . . 56 x 16

m per landing gear, lb/ft 280,180

r 1.21

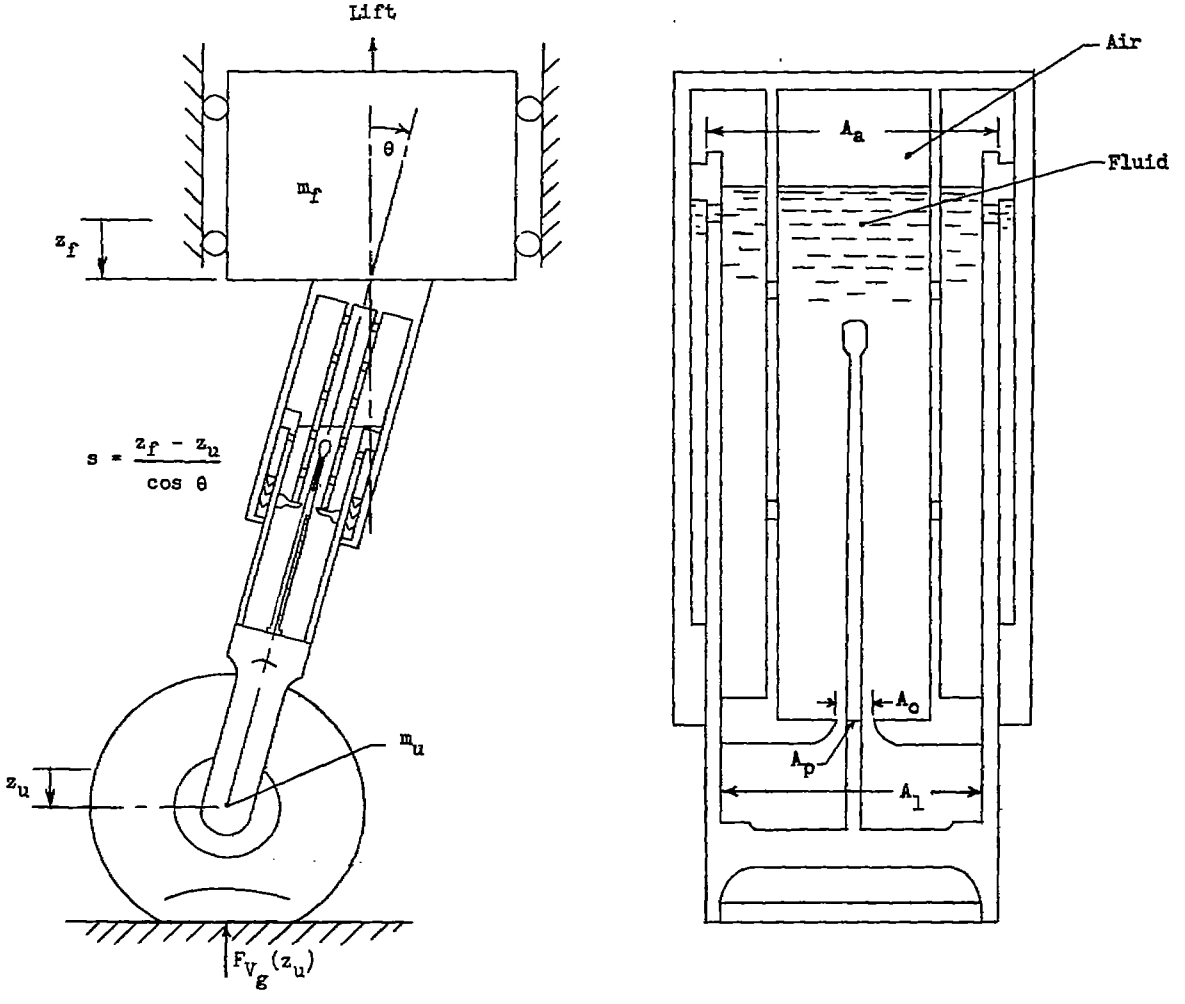

(a) System with two degrees of freedom.

(b) Schematic representation of shock strut.

Figure 1.- Dynamical system (rigid airplane) considered in reference 6.

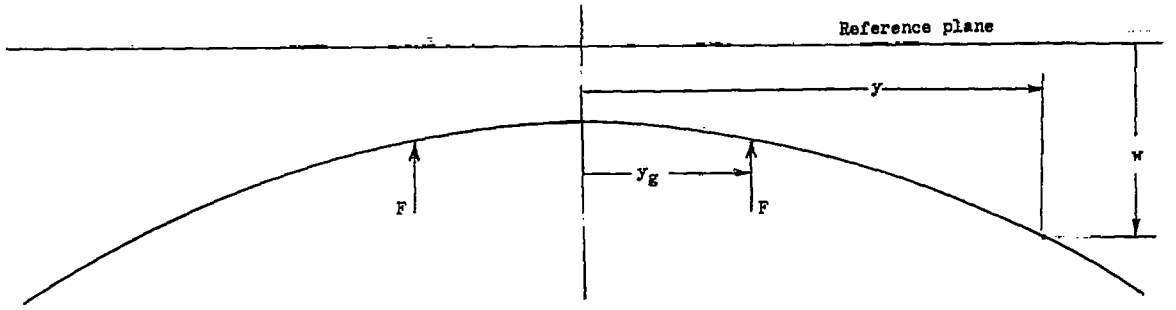

(a) Coordinates along elastic axis.

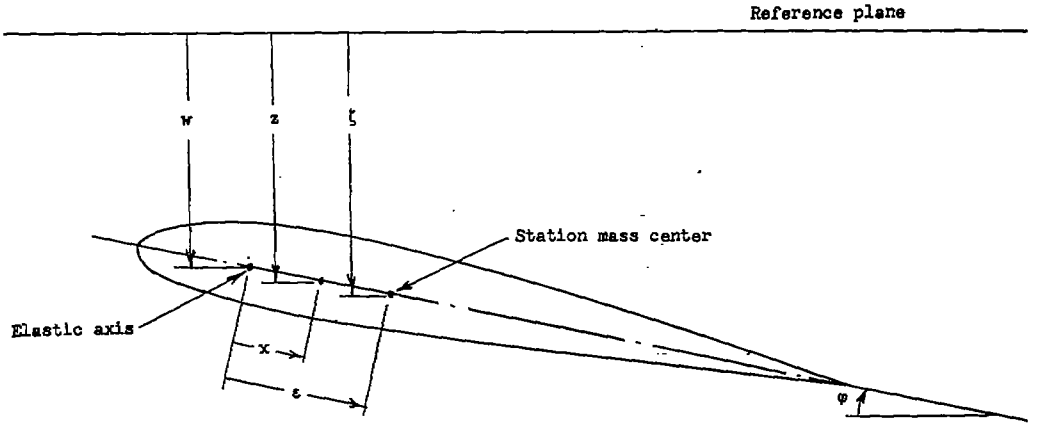

(b) Coordinates at any transverse station.

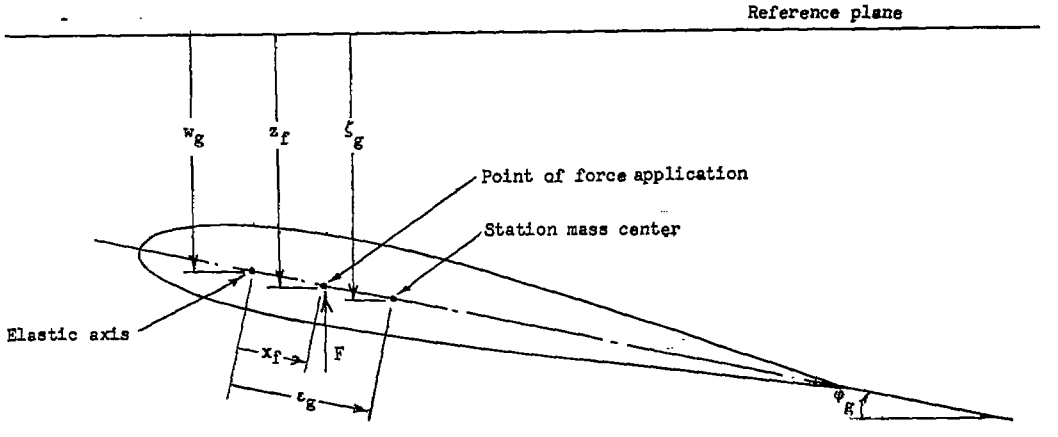

(c) Coordinates at landing-gear station.

Figure 2.- Coordinates for airplane structure.

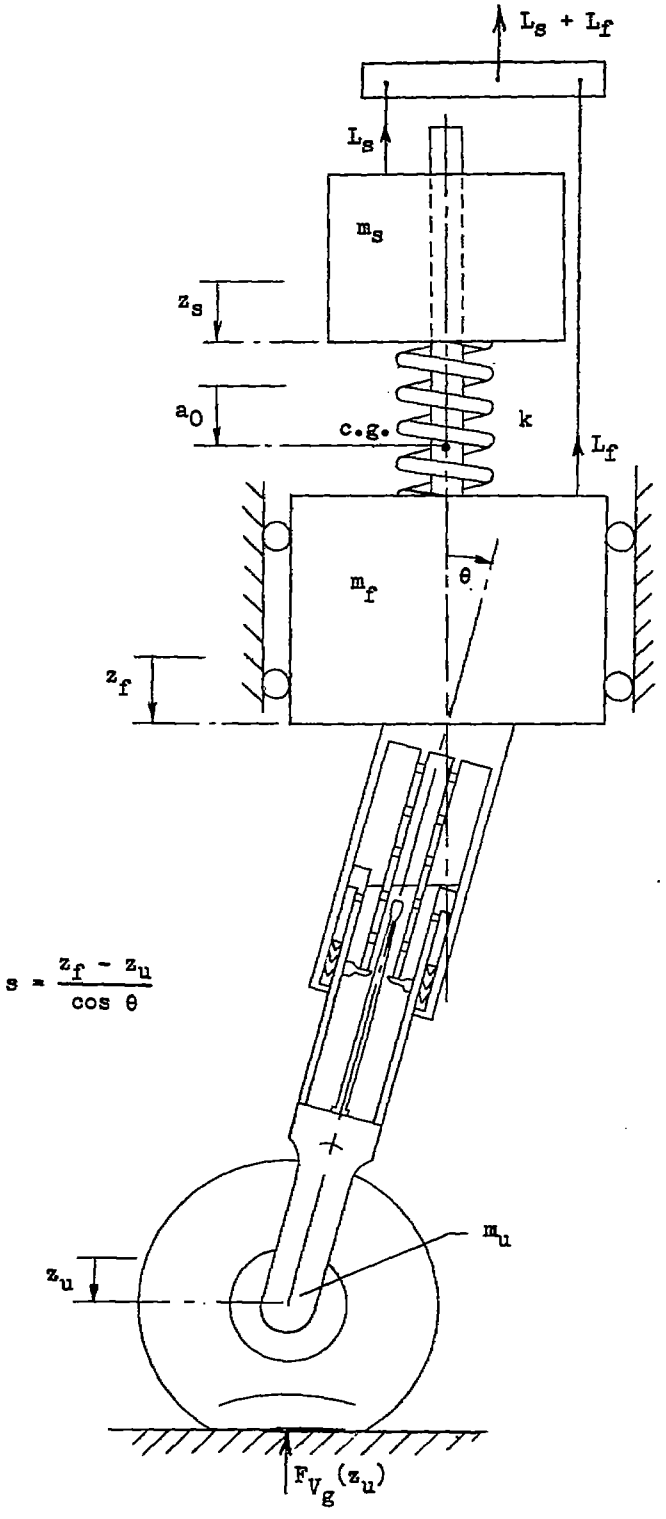

Figure 3.- Equivalent three-mass system for representing flexible airplane and landing gear.

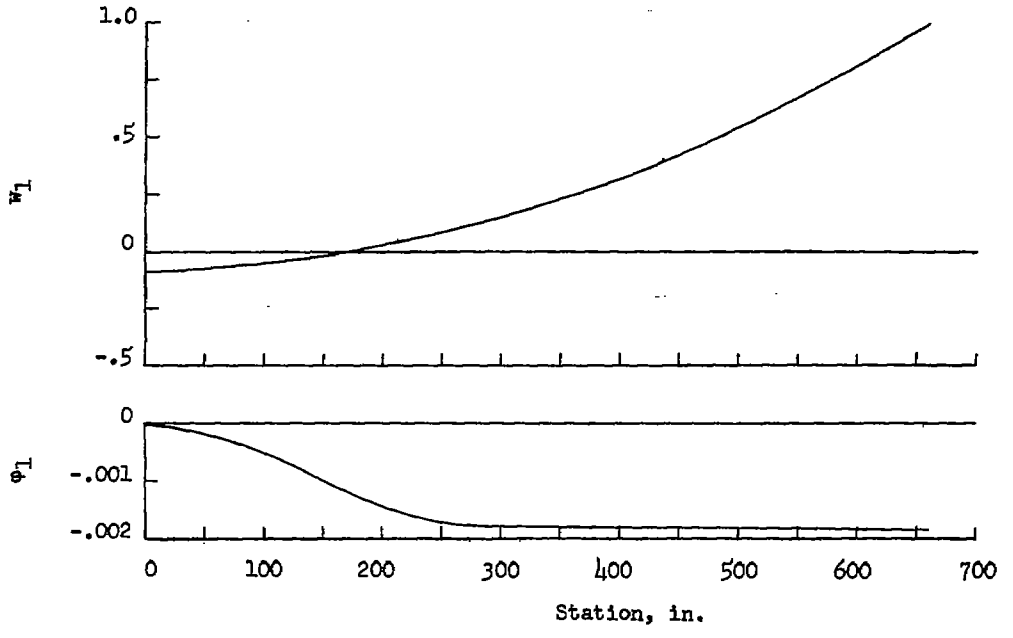

(a) Airplane A.

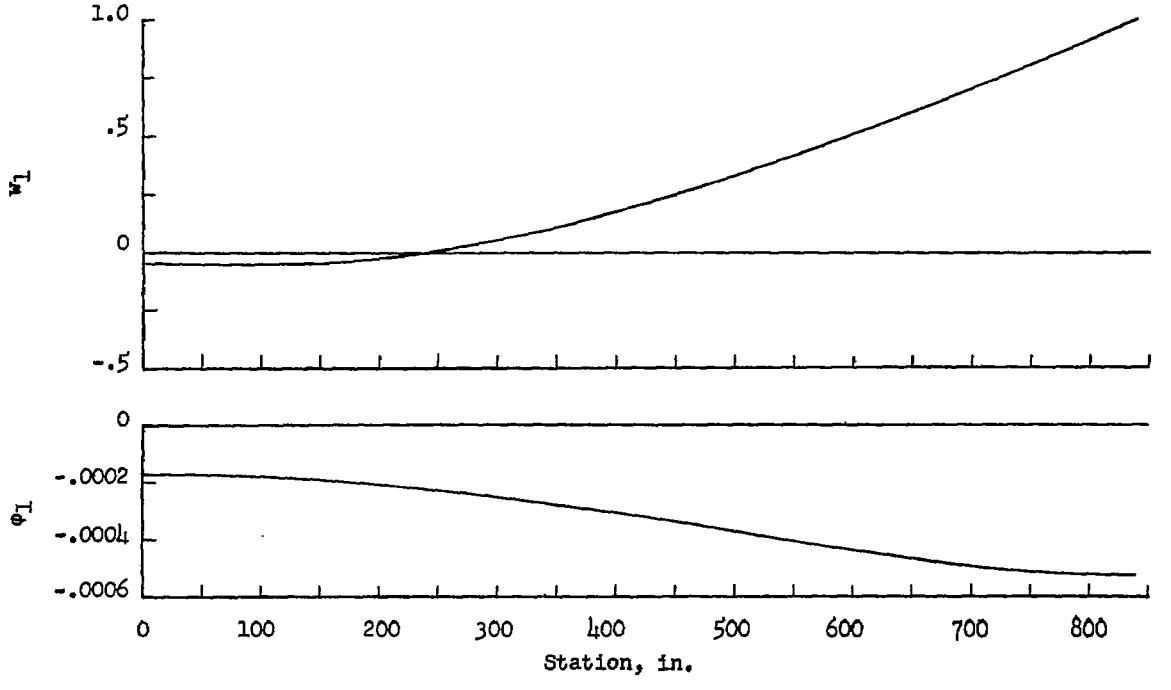

(b) Airplane B.

Figure 4.- Modal functions for bending and torsion.

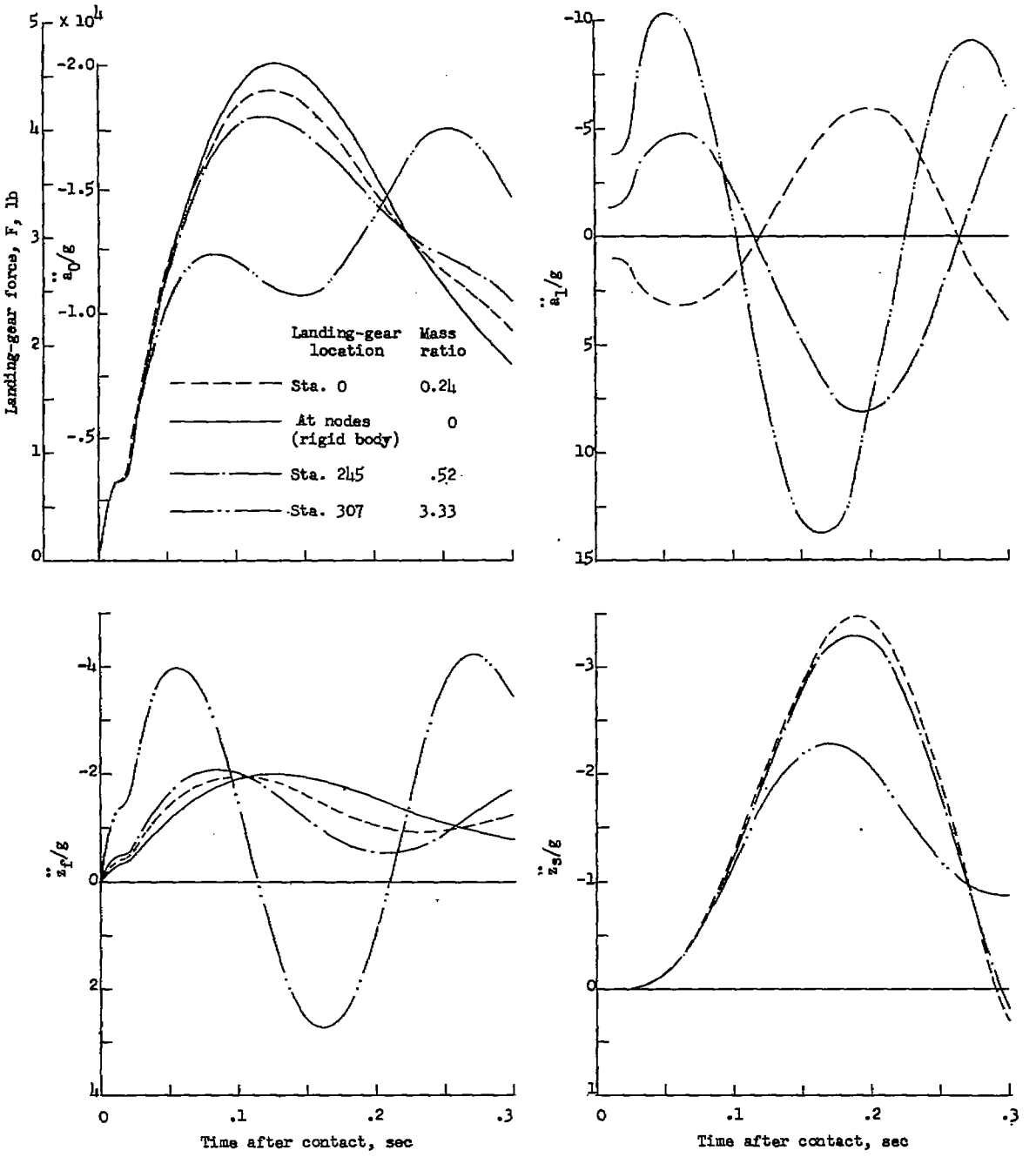

Figure 5.- Time histories of motions of airplane A during impact.

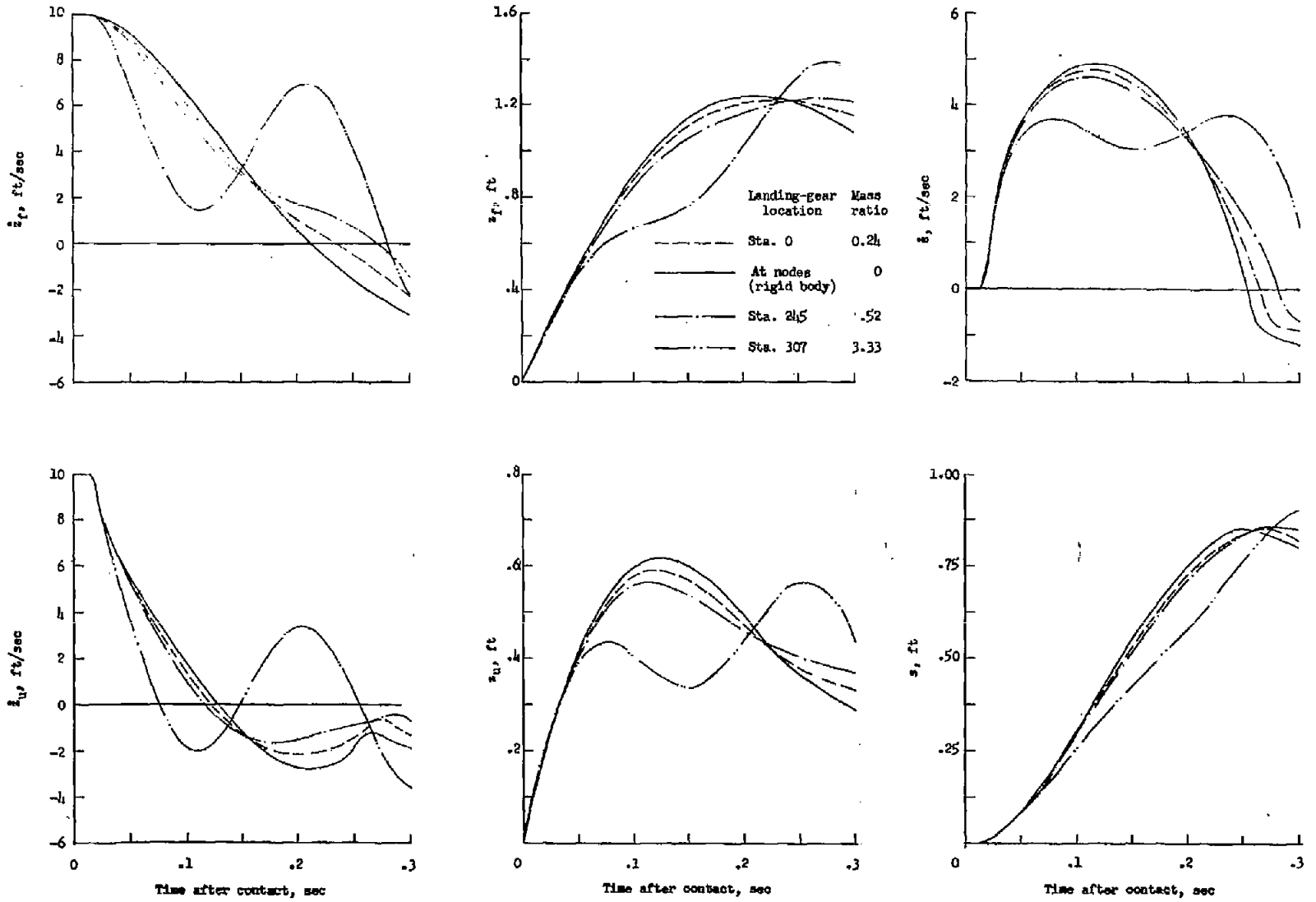

Figure 5.- Concluded.

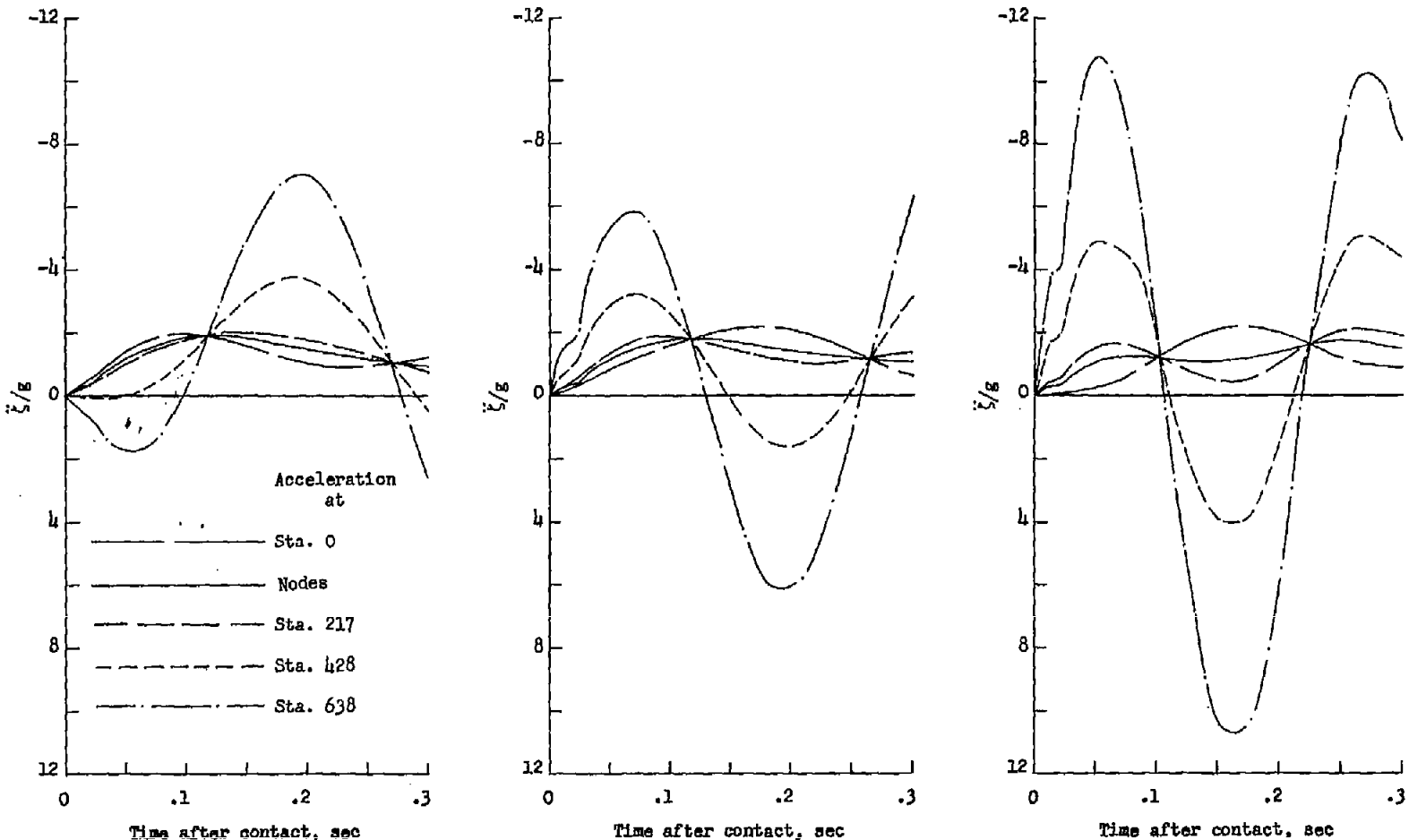

(a) Landing gear at station 0. (b) Landing gear at station 245. (c) Landing gear at station 307.

Figure 6.- Time histories of accelerations at various stations along the span of airplane A.

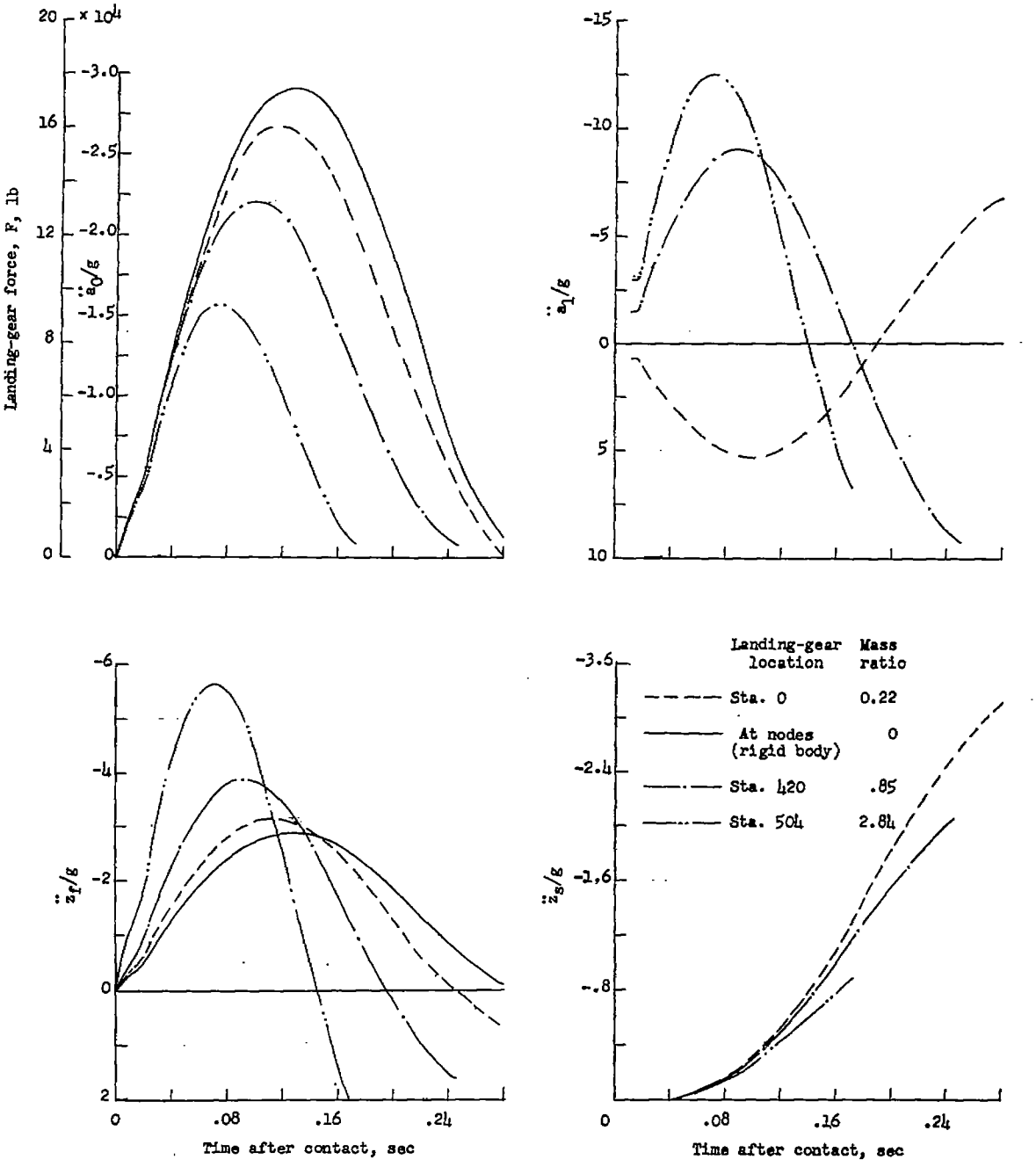

Figure 7.- Time histories of motions of airplane B during impact.

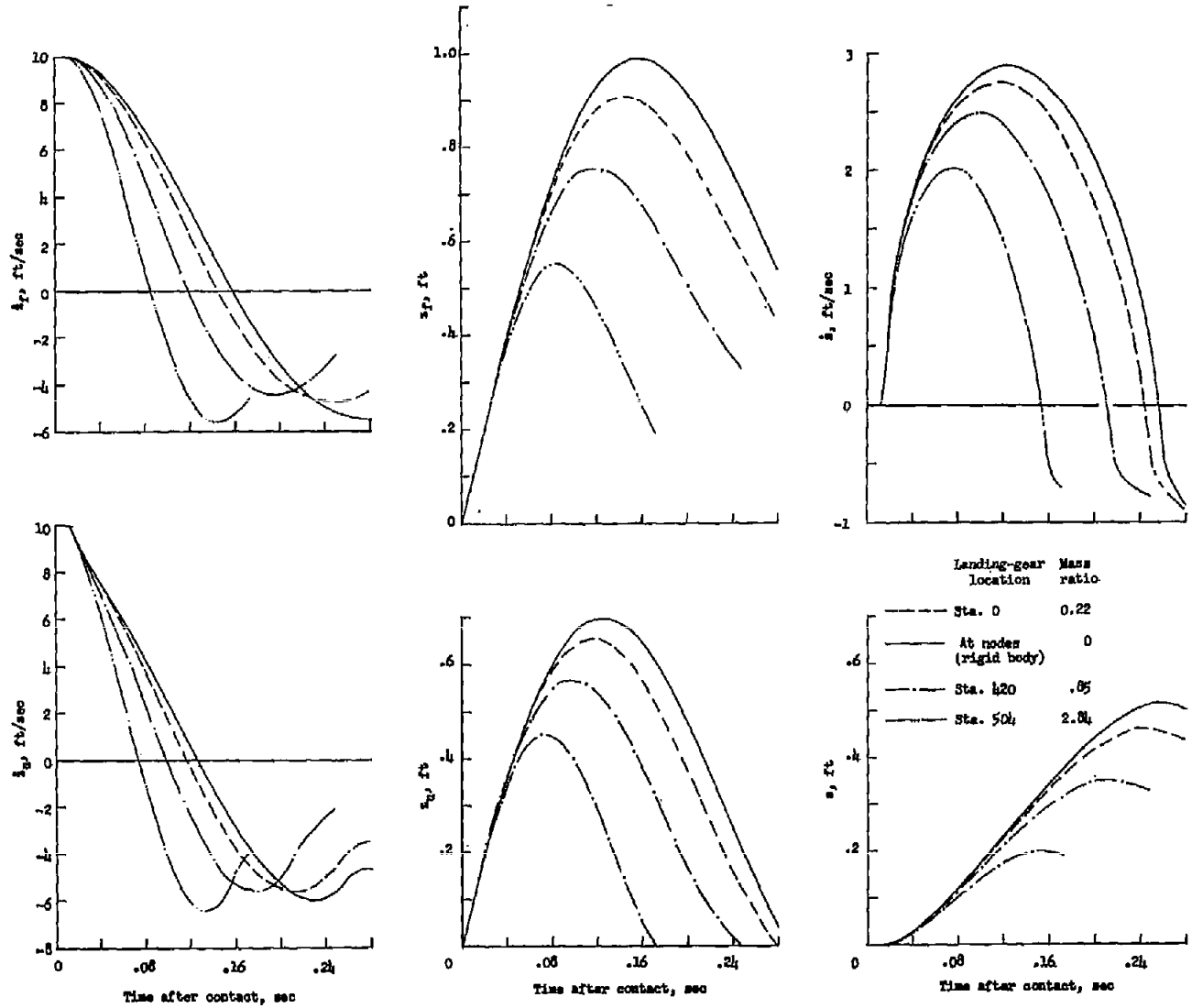

Figure 7.- Concluded.

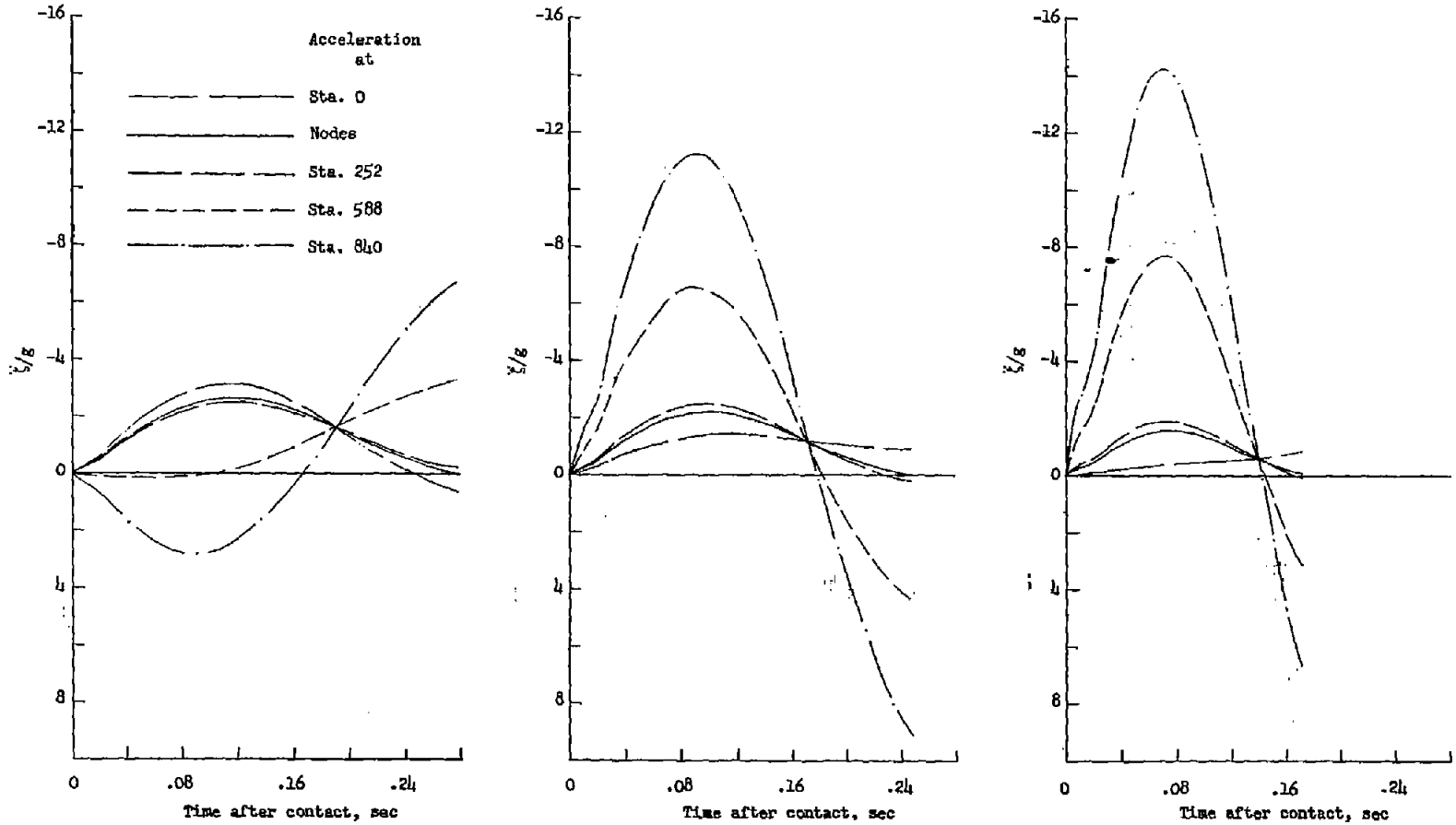

(a) Landing gear at station 0. (b) Landing gear at station 420. (c) Landing gear at station 504.

Figure 8.- Time histories of accelerations at various stations along the span of airplane B.

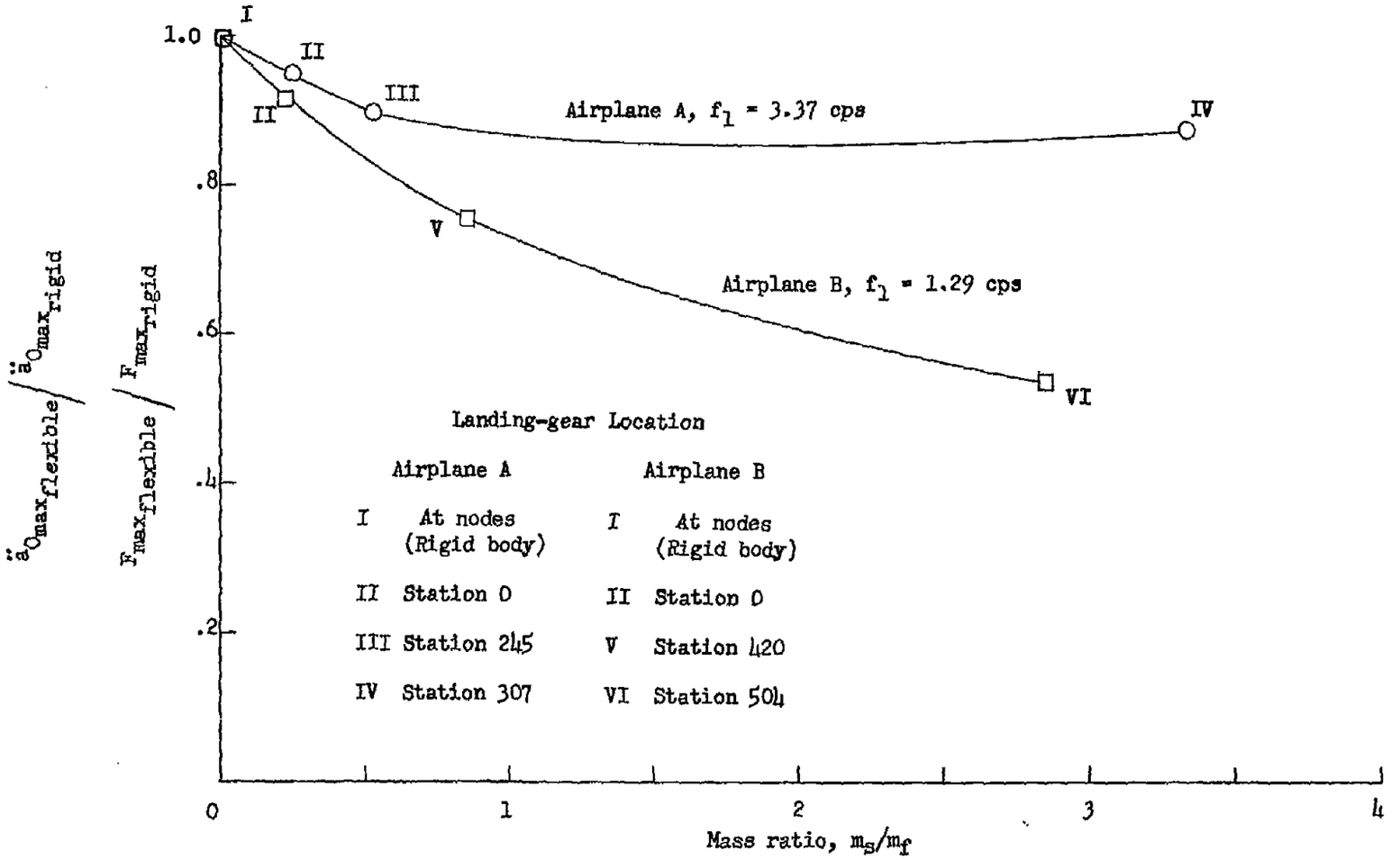

(a) Landing-gear force.

Figure 9.- Effects of interaction.

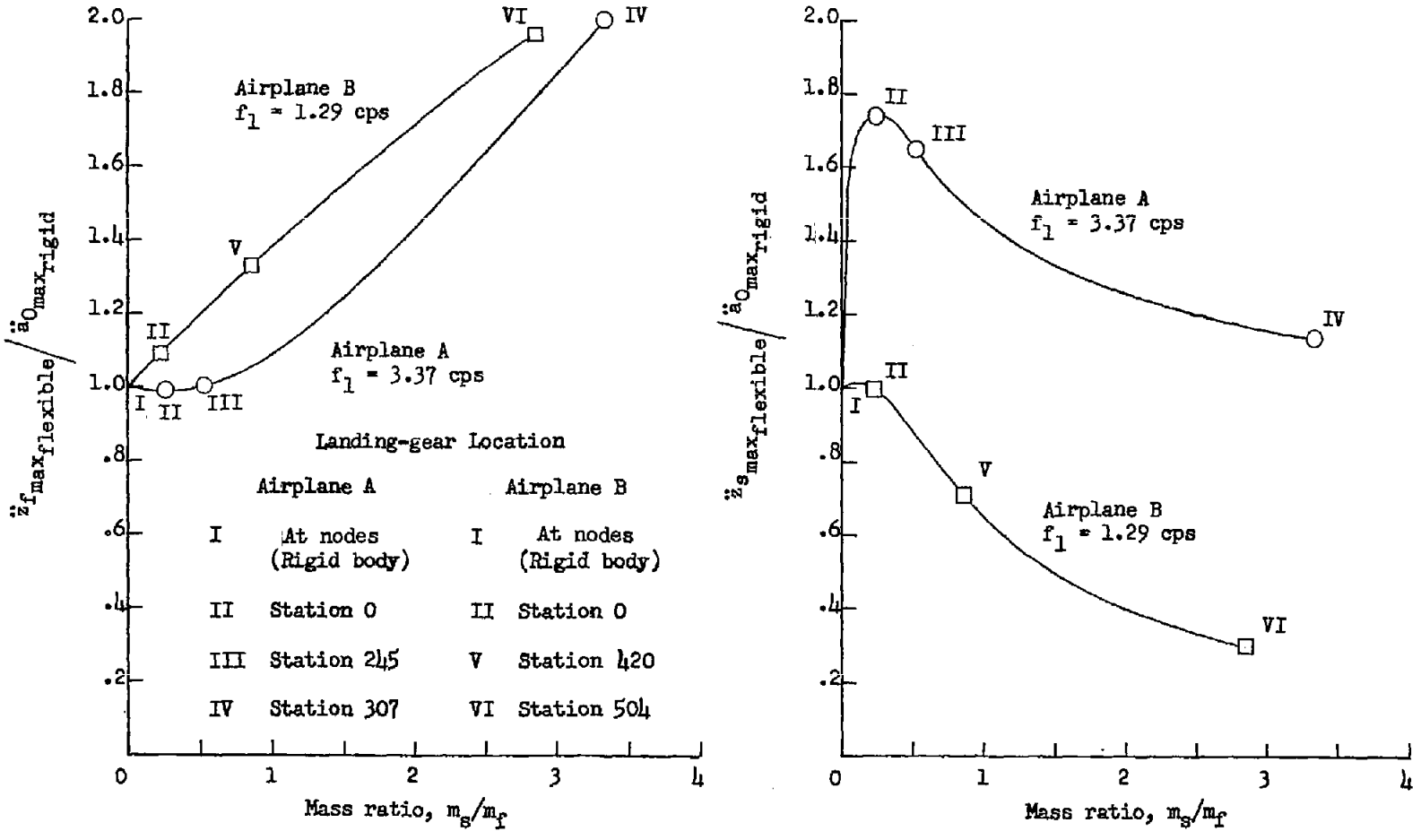

(b) Accelerations of landing-gear attachment point and elastically connected mass.

Figure 9.- Concluded.

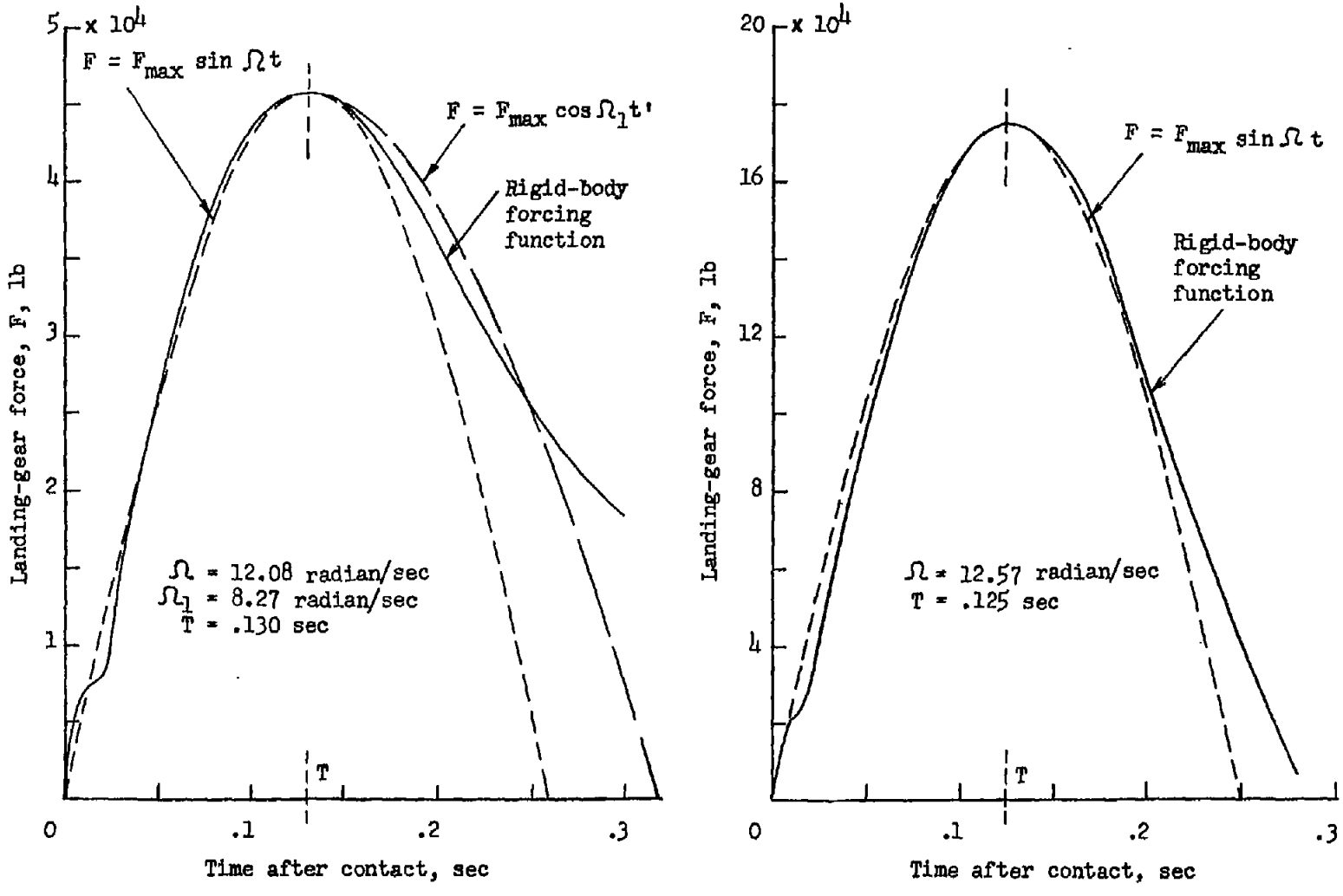

(a) Airplane A.

(b) Airplane B.

Figure 10.- Rigid-body forcing functions and simple analytical approximations.

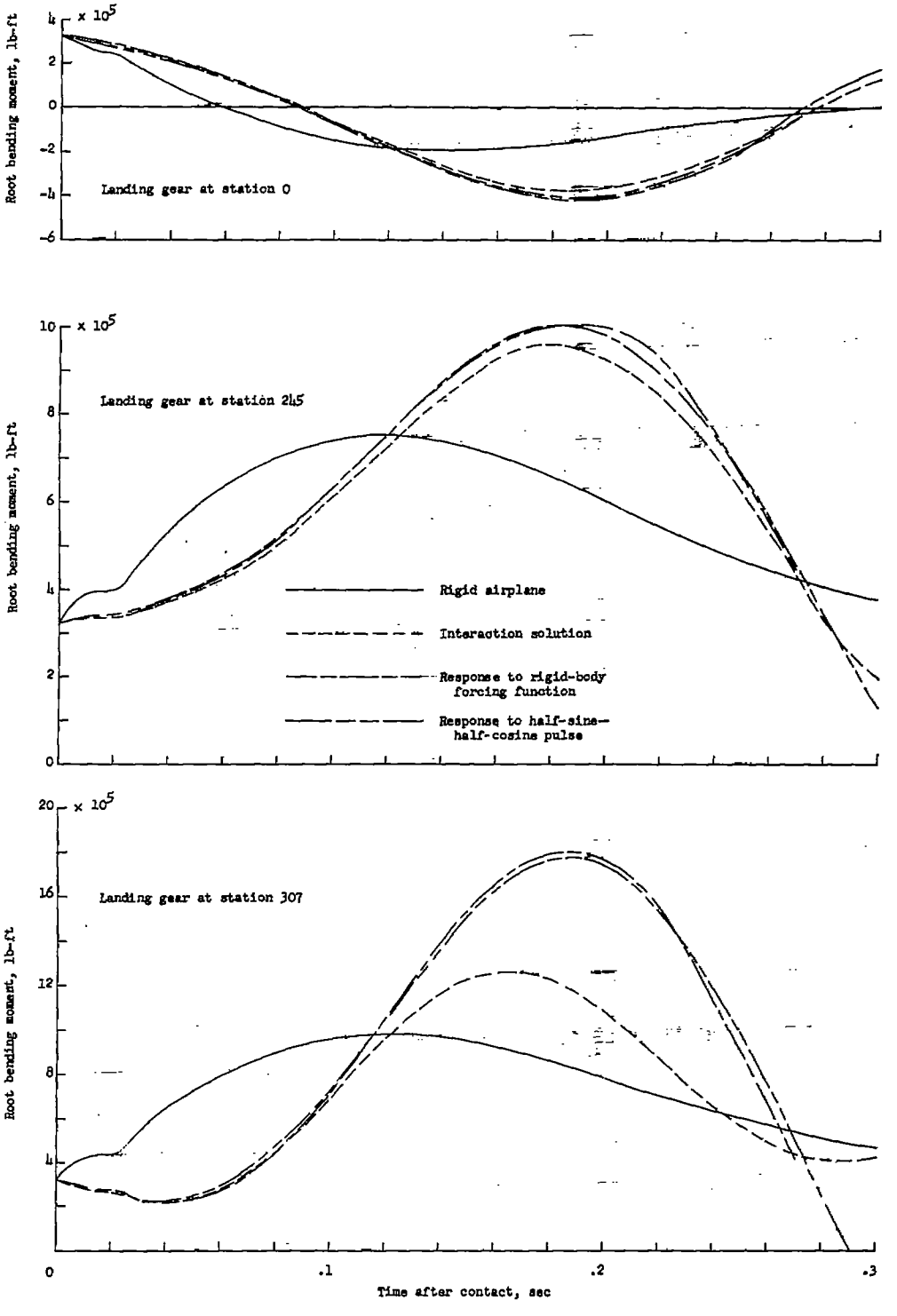

(a) Bending moments.

Figure 11.- Dynamic loads in airplane A.

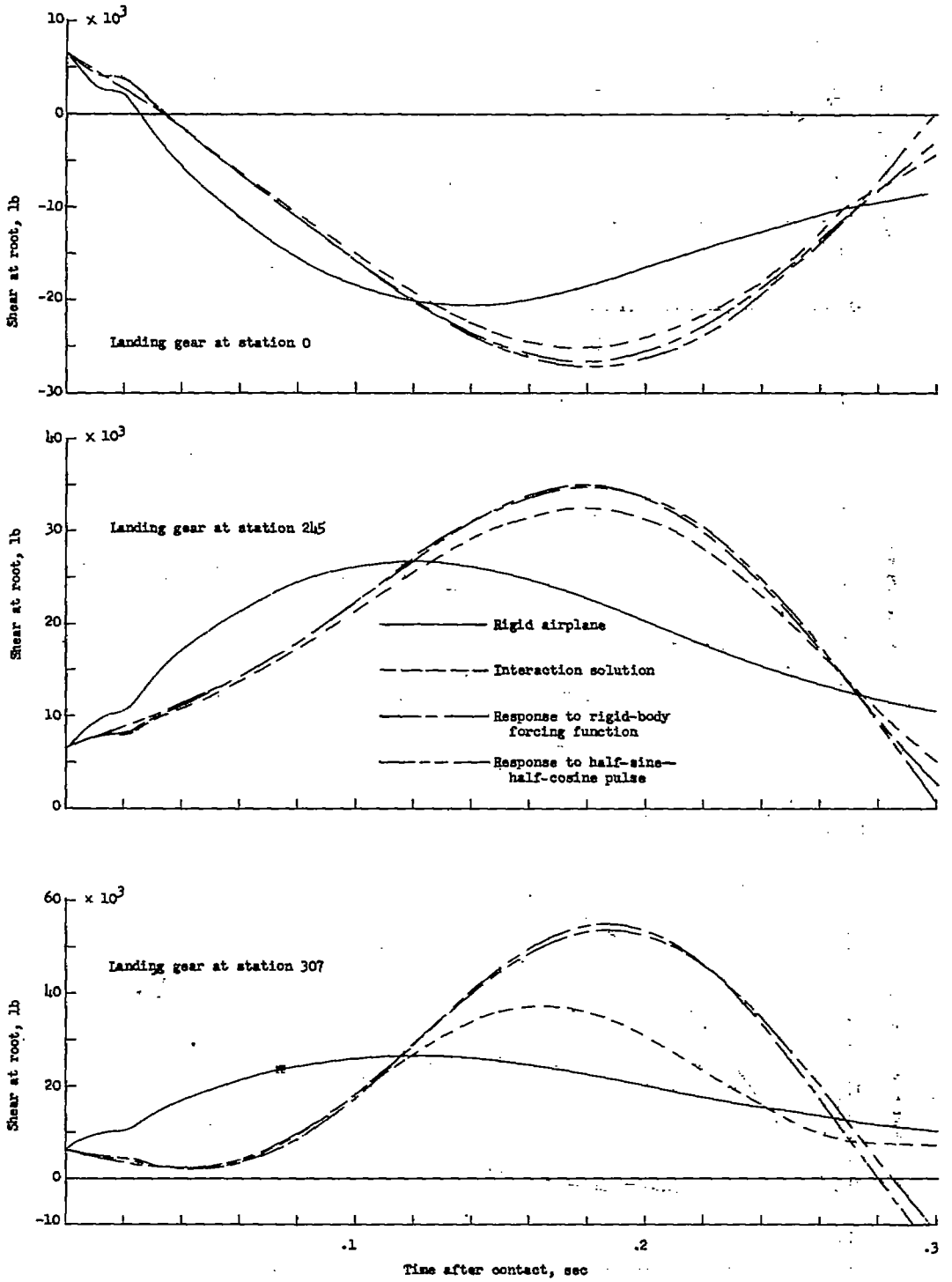

(b) Shears.

Figure 11.- Concluded.

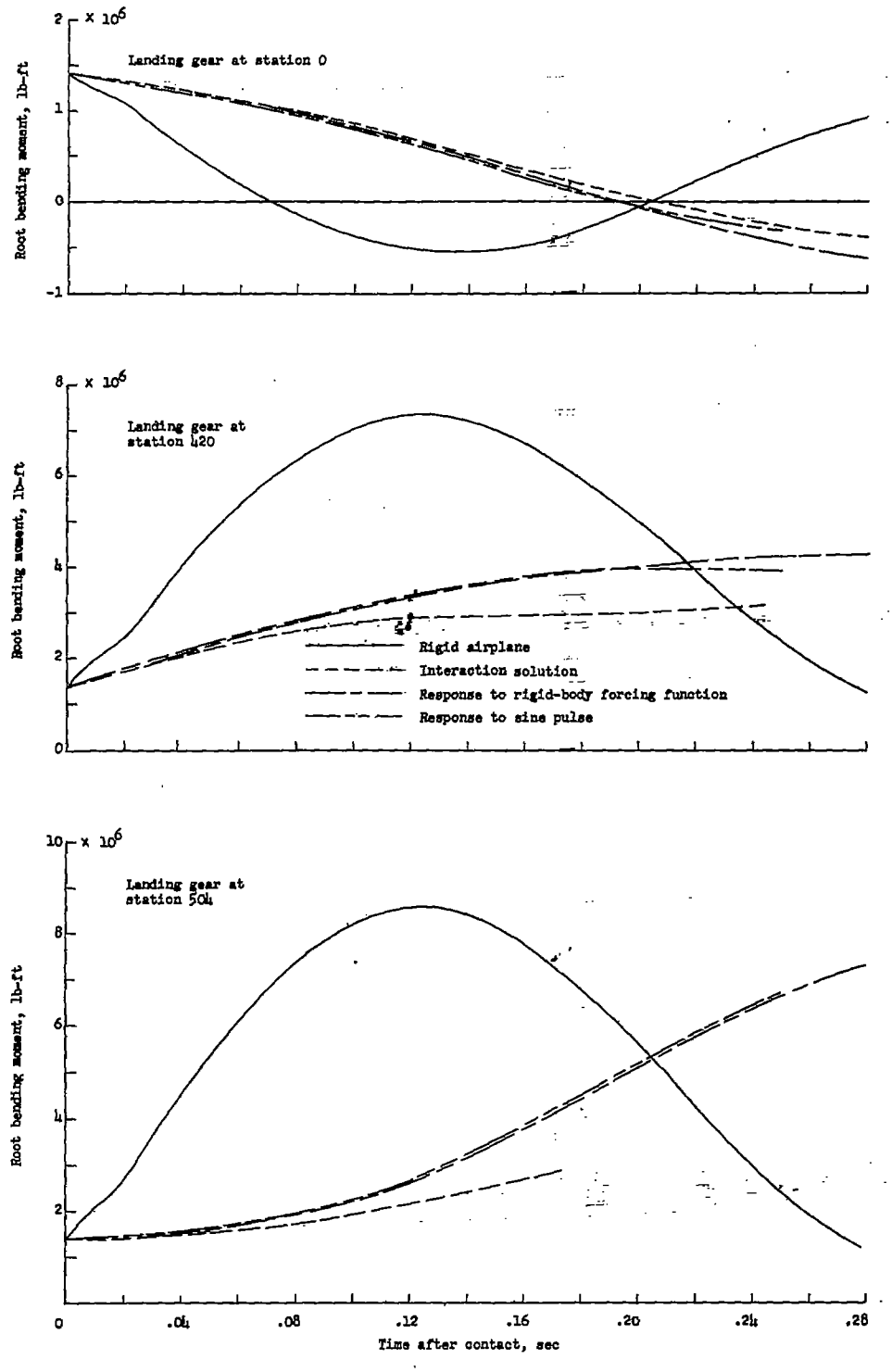

(a) Bending moments.

Figure 12.- Dynamic loads in airplane B.

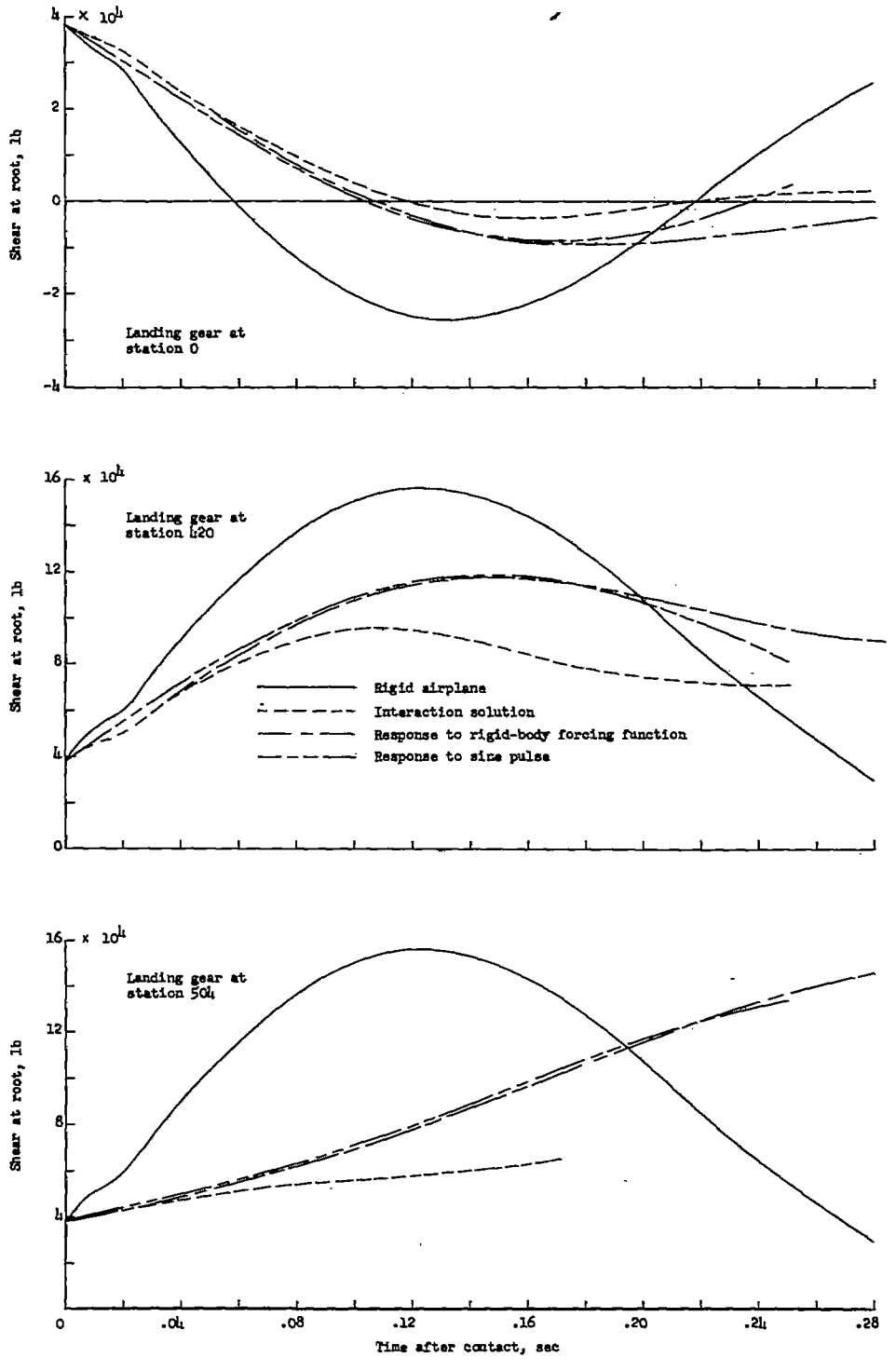

(b) Shears.

Figure 12.- Concluded.